Supporting Information

Accelerated and Controlled Polymerization of Tryptophan *N*-Carboxyanhydride

*Chenlin Ji[1, 2], Tingting Cao[2], Luyao Wang[2, 4], Zhuohang Zhou[2, 4], Yu Zhao[2, 4], Xingliang Liu[2, 4, 6], Chengjie Sun[2, 4, *], Ziyuan Song[5, *], and Jianjun Cheng[2, 3, 4, *]*

[1] School of Materials Science and Engineering, Zhejiang University, Hangzhou, Zhejiang 310058, China.

[2] Department of Materials Science and Engineering, Westlake University, Hangzhou, Zhejiang 310030, China.

[3] Research Center for Industries of the Future, Westlake University, Hangzhou, Zhejiang 310030, China.

[4] Institute of Advanced Technology, Westlake Institute for Advanced Study, Hangzhou, Zhejiang 310024, China.

[5] Institute of Functional Nano & Soft Materials (FUNSOM), Jiangsu Key Laboratory for Carbon-Based Functional Materials and Devices, Soochow University, Suzhou, Jiangsu 215123, China.

[6] Department of Biomedical Engineering, School of Engineering, China Pharmaceutical University, Nanjing, Jiangsu 211198, China

*Corresponding email: chengjianjun@westlake.edu.cn; zysong@suda.edu.cn; sunchengjie@westlake.edu.cn.

Table of Contents

Materials

All commercial reagents were purchased from Shanghai Aladdin Biochemical Technology Co., Ltd. (Shanghai, China) and used as received unless otherwise specified. Amino acid, 18-crown 6-ether (CE), and *N,N'*-bis[3,5-bis(trifluoromethyl)phenyl]thiourea (TU-S) were purchased from Tokyo Chemical Industry (Shanghai, China). 3-(1-Naphthyl)-$_L$-alanine was purchased from Inno-chem Industry (Beijing, China). Triphosgene, 1,3-dimethyl-2-(diethylamino)-2-(*tert*-butylimino)-1,3-diaza-2-phospha(V)cyclohexane (BEMP) and indole were purchased from Shanghai Macklin Biochemical Technology Co., Ltd. (Shanghai, China). The initiator *n*-hexylamine (Hex-NH_2) was purchased from Millipore Sigma Chemical Co. (St. Louis, USA). Deuterated solvents were purchased from Cambridge Isotope Laboratories, Inc. (Tewksbury, USA). The amino acid *N*-carboxyanhydride (NCA) monomers, including γ-benzyl-$_L$-glutamate NCA (BLG-NCA), N^{ε}-benzyloxycarbonyl-$_L$-lysine NCA (ZLL-NCA), N^{ε}-*tert*-butoxycarbonyl-$_L$-lysine NCA (BLL-NCA), γ-tert-butyl-$_L$-glutamate NCA (tBuLG-NCA), $_L$-tryptophan NCA ($_L$-Trp NCA) and $_D$-tryptophan NCA ($_D$-Trp NCA) were synthesized following literature procedures.[1,2]

Instrumentations

NMR

^{1}H nuclear magnetic resonance (NMR) and ^{13}C NMR spectra were recorded on a 600 MHz Bruker BioSpin AVANCE NEO NMR Spectrometer. NOESY experiments were performed with the "noe syesgpph" pulse sequence employing excitation sculpting with gradients for water suppression. 2D data were collected with eight repeated scans, 2048 data points in the direct dimension and 256 increments in the indirect dimension. Unless otherwise noted, a relaxation delay of 3 s was used. The mixing time was set to be 0.3 s. Solid state ^{13}C cross-polarization (CP) magic angle spinning (MAS) NMR experiments were performed on a 500 MHz Bruker Avance NEO spectrometer

equipped with a 3.2 mm HFX triple-resonance MAS probe. A magic-angle spinning speed of 10 kHz was used for all experiments. The initial 90° pulse length was 3.0 μs, and a recycle delay of 2 s was used. The duration of the ramped CP pulse was 2 ms. Chemical shifts (δ) were reported with the residual protons in deuterated solvents as reference. MestReNova software (version 14.0.0, Mestrelab Research, Escondido, CA, USA) was used for all NMR analysis.

X-Ray diffraction

Single crystals of Trp-NCA were selected and characterized on a Bruker D8 Venture diffractometer. The crystal was kept at 100.00 K during data collection. The data were processed in Olex2,[3] the structure was solved with the XT[4] structure solution program using Intrinsic Phasing and refined with the XL[5] refinement package using Least Squares minimisation.

GPC

Gel permeation chromatography (GPC) experiments were performed on a system equipped with an isocratic pump (1260 Infinity II, Agilent, Santa Clara, USA), a multi-angle laser light scattering (MALLS) detector (DAWN HELEOS-II, Wyatt Technology, Santa Barbara, USA), and a differential refractive index (dRI) detector (Optilab, Wyatt Technology, Santa Barbara, USA). The detection wavelength of HELEOS was set at 658 nm. Separations were performed using serially connected size exclusion columns (three Shodex packed columns KD-803, KD-804 and KD-805, 10 μm, 8 × 300 mm, Yokohama, Japan) using DMF containing LiBr (0.1 M) as the mobile phase at a flow rate of 1.0 mL/min at 50 °C. The MALLS detector was calibrated using pure toluene and was used for the determination of the absolute molecular weights (MWs). The MWs of polymers were determined based on the dn/dc value of each polymer sample using the internal calibration system processed by the ASTRA software (Version 8.12, Wyatt Technology, Santa Barbara, CA, USA).

FTIR

Fourier transform infrared (FTIR) spectra were recorded on a Perkin Elmer 100 serial spectrometer with a diamond ATR element. FTIR spectrophotometer (PerkinElmer, Santa Clara, CA, USA) was calibrated with polystyrene film. IR spectra were obtained with 1 cm^{-1} resolution and 32 scans.

LC MS

The purity of Nap-NCA was assessed by LC MS. A minimal amount of NCA was dissolved in 80% acetonitrile in water (0.4 mL) containing 0.1% formic acid (FA) and analyzed on an LC system (VanquishFlex, Thermo-Fisher) equipped with a Phenomenex Luna C18(2) column (100 Å, 5 μm, 50 × 2 mm, 0.3 mL/min) and connected to a diode array detector (DAD) and an Ultra-performance liquid chromatography-time of flight mass spectrometer (UPLC-TOF MS) (Syanpt-XS, Waters). All ions were analyzed in positive mode.

MALDI-TOF MS

Matrix-assisted laser desorption/ionization time-of-flight (MALDI-TOF) mass spectra were collected on a Bruker Rapiflex in the mass spectrometry laboratory, Westlake University, with tetrahydrofuran as solvent and 2,5-dihydroxybenzoic acid (DHB) as the matrix. All polypeptide samples or the matrices/salts were dissolved in THF at a concentration of 10 mg/mL. The “sandwich” technique was used for MALDI-TOF MS sample preparation. Briefly, 0.5 μL matrix solution was deposited on the wells of a 384-well ground-steel plate. Upon brief drying, 0.5 μL sample solution was deposited on top of the dried matrix. Finally, another 0.5 μL of DHB solution was deposited. Data analyses were conducted with Bruker’s flexAnalysis software.

CD

Circular dichroism (CD) measurements were carried out on a chirascan spectrometer V100 (Applied Photophysics, Leatherhead, UK). In short, the solution of polypeptides (0.5 mL, 0.02 mg/mL) was added to the CD cuvette for characterization (path length = 1 mm). The solution of monomers (0.5 mL, 0.05 mg/mL) was added to the CD cuvette for characterization (path length = 1 mm). The mean residue molar ellipticity was calculated based on (1) as follows:

$$[\theta] = (\theta \times M)/(l \times c) \quad (1)$$

where θ is the raw ellipticity from CD measurement, l is the path length, and M and c are the mean residue MW and concentration of the monomers and polypeptides, respectively.

HRTEM

HRTEM images were obtained using a Talos F200X G2 microscope operated at an accelerating voltage of 200 kV. Standard TEM samples were prepared by dropping diluted polymer solutions onto carbon film-coated copper grids. The excess solutions on the grids were removed using filter paper and the residues were allowed to dry under ambient condition. For negatively stained samples, the sample solutions loaded on TEM grids were rinsed by 50 μL of 0.5 wt% uranyl acetate solution and then blotted by filter paper followed by drying under ambient condition. The carbon film-coated copper grids (carbon film 300 mesh copper, China Mirror Science Instrument, China) were pre-treated with plasma for 15 s before loading samples.

PL

Fluorescence emission and excitation spectra were measured in quartz cells with a path length of 1 mm on a FLS1000 spectrofluorometer (Edinburgh) equipped with a Xenon lamp. The 3D spectra were recorded at λ_{ex} from 240 nm to 400 nm and λ_{em} from 250 nm to 500 nm.

Methods

Polymerization kinetics

To record the polymerization kinetics, the consumption of NCA was monitored through FTIR or NMR. For FTIR analysis, the kinetics was monitored *in situ* in a liquid cell (for reactions in DCM solutions) or on an ATR FTIR plate after drying (for reactions in DMF/DCM cosolvents). Typically, the polymerization mixture was immediately transferred into a liquid FTIR cell after the mixing of reactants. The FTIR spectra were monitored at different time intervals until the disappearance of anhydride peaks at 1850 cm^{-1} and 1774 cm^{-1}. The concentration of NCA monomer was then quantified through the standard curve based on the absorbance at 1774 cm^{-1}. For BLG-NCA, 1730 cm^{-1} was used as the internal standard for calculation of monomer conversions. For Trp-NCA, the absorption peak at 746 cm^{-1} (assigned to the trisubstituted benzene ring) and the υ(C=C) stretching vibration peak at 1458 cm^{-1} were used as internal references.

For NMR analysis, the kinetics was monitored in deuterated solvent in NMR tubes. The mixture was vortexed and transferred into an NMR tube, and the NMR spectra were collected at different time intervals. The conversions of NCA were quantified by monitoring the integrals of ring N-H signals (δ = 10.9 - 11.1 ppm) or α-H (δ = 4.6 ppm). The ring N-H signal at t = 0 was calculated based on the integral ratio of side-chain indole N-H peaks between Trp-NCA (δ = 11.04 ppm) and resulting PLW (δ = 10.44 ppm).

In order to determine molecular weights (MWs) at different monomer conversions, the polymerization was quenched at designated time intervals by adding trifluoroacetic acid (TFA, 2.5 vol%). The resulting polypeptides were collected by precipitation, dried, and redissolved in DMF containing LiBr (0.1 mol/L) for GPC analysis.

Synthesis of Nap-NCA

To a pressure vessel with a heavy wall, L-1-naphthylalanine (3.0 g, 13.9 mmol, 1.0 eq), THF (50 mL), methyloxirane (9.7 mL, 139 mmol, 10 eq) were added sequentially under magnetic stirring. Triphosgene (2.1 g, 7.1 mmol, 0.5 eq) was added in one portion and the vessel was sealed immediately. The amino acid solids gradually dissolved within ~60 min with noticeable heat release. The reaction was stirred at room temperature for ~4 h in total and cooled down to ~4 °C in an ice bath. The excessive triphosgene was quenched by adding cold water (20 mL) at ~4 °C. The mixture was extracted with ethyl acetate (EA, 30 mL × 2) at room temperature. The combined organic phase was washed with brine and dried with anhydrous Na_2SO_4. After the removal of the solvent by rotatory evaporation under vacuum, the crude product was purified by crystallization in hexane/THF below 10 °C. The Nap-NCA was obtained as a white needle crystal (1.55 g, 46.3%). The NCA can be stored at -10 °C for at least 5 months.

^{1}H NMR (600 MHz, DMSO-d_6) δ 9.04 (s, 1H), 8.09 (d, J = 8.4 Hz, 1H), 7.95 (d, J = 7.6 Hz, 1H), 7.87 (d, J = 8.2 Hz, 1H), 7.62 – 7.57 (m, 1H), 7.57 – 7.52 (m, 1H), 7.50 – 7.46 (m, 1H), 7.42 (d, J = 6.3 Hz, 1H), 4.85 (s, 1H), 3.60 (dd, J = 14.6, 5.4 Hz, 1H), 3.50 (dd, J = 14.6, 7.2 Hz, 1H).

^{13}C NMR (151 MHz, DMSO-d_6): δ 170.9, 151.8, 133.5, 131.6, 131.5, 128.7, 127.7, 126.3, 125.5, 123.7, 57.9, 33.5.

HRMS (ESI−EIC, m/z): $[M + H]^+$ calcd for $C_{14}H_{11}NO_3$: 242.0812; found: 242.0821.

FTIR (cm^{-1}): 1854, 1781, 1597.

General procedures for open vessel NCA polymerization

A typical polymerization procedure was as follows. To a DMF/DCM solution (1:1, v/v, 197.2 μL) of Trp-NCA (10 mg, 0.043 mmol), stock solution of Hex-NH_2 (0.076 M, 11.2 μL) and DMAP (0.1 M, 8.69 μL) were added sequentially to initiate the polymerization.

Final condition: $[M]_0$ = 0.2 M, $[M]_0/[I]_0$ = 50, and $[I]_0/[DMAP]_0$ = 1. The reaction was conducted in an open vessel under ambient atmosphere. After completion, the polypeptide was isolated by precipitation into cold diethyl ether, dried under vacuum, and subsequently dissolved in DMF containing 0.1 M LiBr for GPC analysis.

The control polymerization in the absence of any catalyst was performed in a similar way, but without the addition of DMAP.

The polymerization in the presence of DMAP/AcOH was conducted in a similar way, but under anhydrous conditions. The solutions of Trp-NCA (10 mg, 0.043 mmol) and AcOH (2.5 ul, 0.044 mmol) were first mixed, followed by the addition of initiators and DMAP. ($[M]_0/[AcOH]_0$ = 1).

The preparation of random copolypeptides was conducted through simultaneous addition of monomers. Meanwhile, the block copolypeptides were synthesized with a sequential addition of monomers.

The relative secondary structure content in our copolypeptide solid powder was determined by employing FTIR deconvolution for the peaks within the amide I region (1800-1600 cm^{-1}), adopting standardized methodologies as outlined in literature[6,7]. Specifically, the Peak Analyzer function in Origin software was used for the deconvolution analysis, ensuring a robust and replicable evaluation of the spectral data. Specific peak assignments: 1650-1655 cm^{-1} (α-helix), 1625-1635 cm^{-1} and 1692 cm^{-1} (β-sheet), and 1675 cm^{-1} (β-turn).

General procedure for the deprotection of polypeptides

To remove the side-chain Boc or *t*Bu protecting group in PBLL-*co*-PLW or P(*t*Bu)LG-*co*-PLW, the obtained polypeptide was treated with TFA/TIS/H_2O cleavage solution (95:2.5:2.5, v/v/v, 2 mL) at room temperature for 3 h under gentle shaking. After the removal of TFA, the obtained viscous liquid was dissolved in DMF (0.5 mL) and precipitated in cold ether/hexane (1:1, v/v) for three times. The precipitate was dissolved in 5.0 mL of DMF, dialyzed with a membrane (MWCO 3500) in deionized

water for 3 days and lyophilized to give the deprotected polypeptide in the form of TFA salt. All operations require protection from light.

NMR titration

NMR titration experiments were conducted to probe the molecular interactions between the reactants during NCA polymerization. Taking the experiments to elucidate the AcOH/Hex-NH_2/DMAP interactions as an example, DMAP (24.4 mg, 0.086 mmol) was dissolved in DMF-d_7/CD_2Cl_2 (250 μL), into which Hex-NH_2 (26.4 μL) were added. Various amounts of AcOH solution were then added (from 0 to 572.5 μL), so that the $[AcOH]_0/[Hex\text{-}NH_2]_0$ ratio was 0 to 50. The chemical shifts of ring N-H at different $[AcOH]_0/[Hex\text{-}NH_2]_0$ ratios were recorded.

The fraction of Hex-NH_2 and DMAP protonation was quantified by the chemical shift of α-H of Hex-NH_2, which was calculated according to the following equation:

$$\delta_m = \delta_b + (\delta_s\text{-}\delta_b)\cdot X_s$$

Where δ_b and δ_s are the standard chemical shifts of α-H in the amine (-NH_2) and ammonium (-NH_3^+) forms of Hex-NH_2, respectively, and δ_m is the chemical shift of α-H under certain conditions. The mole fraction of protonated amine, X_s, was then calculated from the equation. [8]

Simulation Methods

All calculations were performed using the Gaussian 16 program package. [9] Geometry optimizations of all reactants, products, intermediates, and transition states were carried out at the B3LYP[10-12]-D3BJ[13-14]/def2-SVP[15] level of theory. Harmonic vibrational frequency calculations were performed at the same level to confirm that each optimized minimum has no imaginary frequencies and that each transition state possesses a single imaginary frequency. Intrinsic reaction coordinate (IRC) calculations were further conducted to verify the correct connectivity between each transition state and the corresponding reactant and product minima. To obtain more accurate electronic

energies, single-point energy calculations were performed on the B3LYP-D3BJ/def2-TZVP[15] level of theory. We reported Gibbs free energies were computed by combining the single-point electronic energies with the Gibbs free energy corrections (thermal and entropic contributions) obtained from the frequency calculations at the optimization level. All calculations were performed in DMF/DCM 1:1 using the PCM solvation model.[16] The 3D structures of key transition states were visualized using CYLview software.[17]

Supporting Scheme

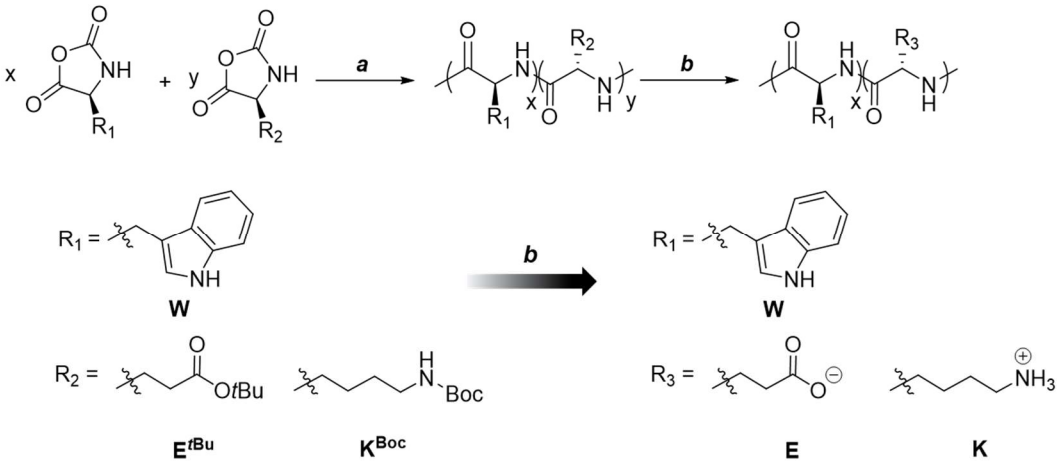

Scheme S1. Preparation of water-soluble statistical Trp-containing copolypeptides. (a) Hex-NH_2, AcOH/DMAP, DCM/DMF, RT. (b) TFA/TIS/H_2O, 0 ºC, 3 h.

Supporting Figures

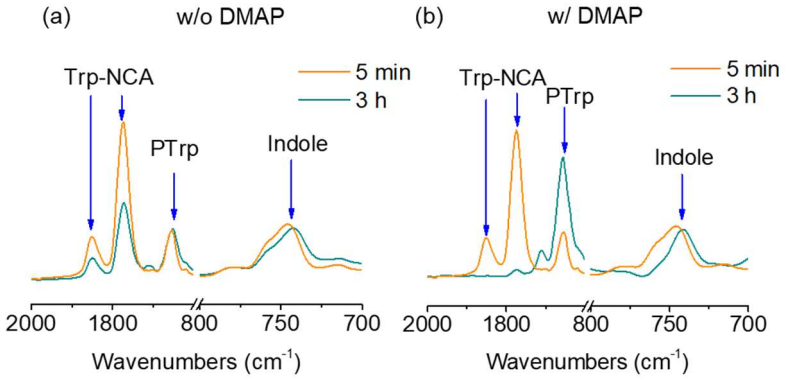

Figure S1. FTIR characterization of polymerization mixture in the absence (a) or presence (b) of DMAP. $[M]_0$ = 0.2 M; $[M]_0/[I]_0$ = 50.

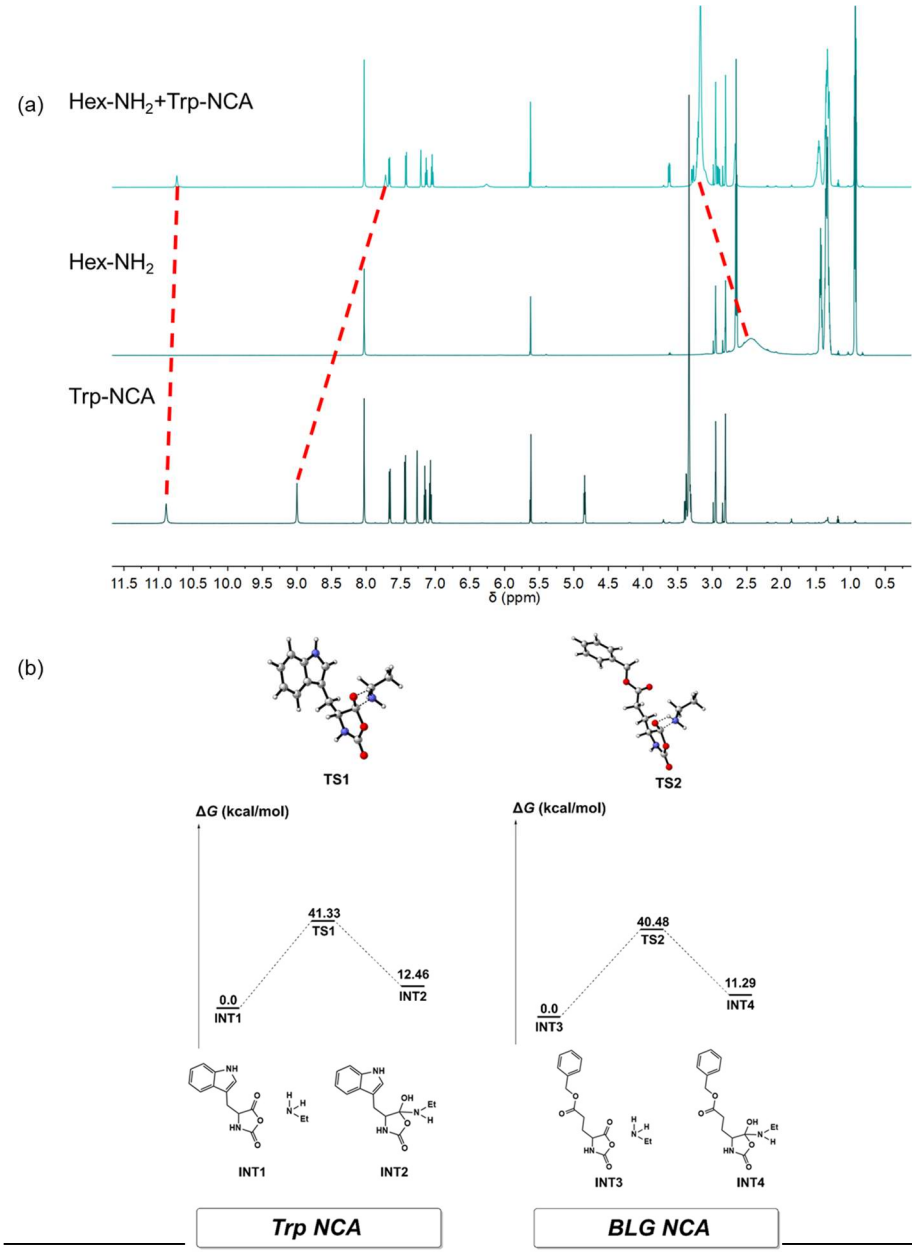

Figure S2. Interactions between side-chain indole and primary amine during the polymerization of Trp-NCA. (a) Overlaid ^{1}H NMR spectra of Trp-NCA, Hex-NH_2 and mixtures. $[\text{Trp-NCA}]_0/[\text{Hex-NH}_2]_0 = 1$. (b) Calculated Gibbs free-energy profile of the model ring opening reaction in different NCA monomers. BLG NCA was used as a model monomer for comparsion. Some crucial intermediates (INT) and transition states (TS) are illustrated by 3D models where some hydrogen atoms are neglected for clarity.

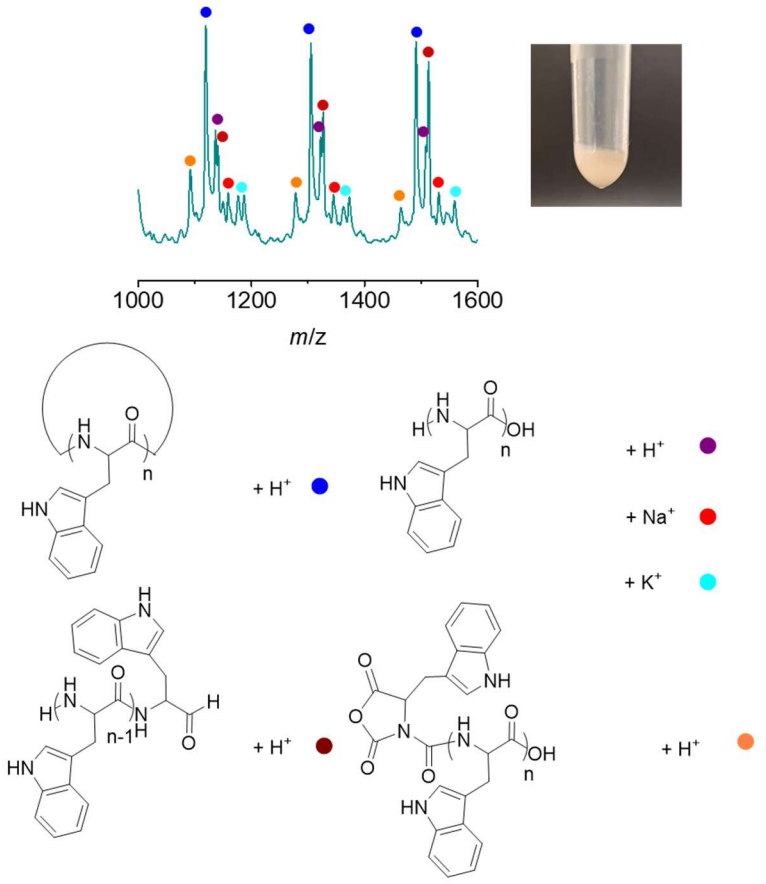

Figure S3. MALDI-TOF MS of the degradation product of Trp-NCA in DMF/DCM cosolvent (1:1, v/v) after 24-h exposure in air. $[M]_0$ = 0.2 M. The obtained *m*/z from major peaks agreed well with the calculated values, including water-initiated polymerization (18.02 + 186.21*n* + 1.01) and cyclic PLW (186.21*n* + 1.01).

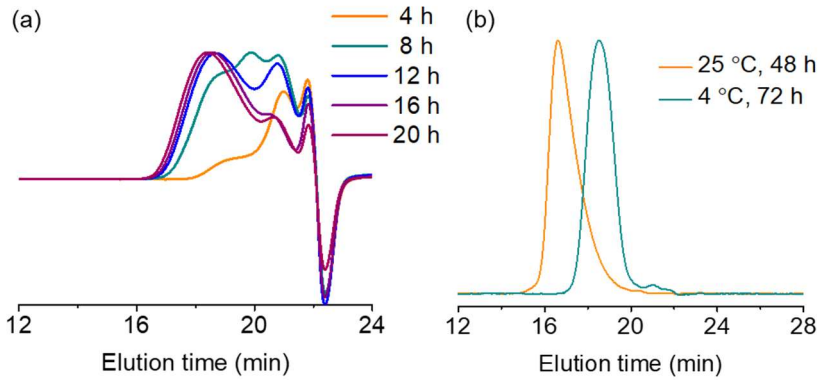

Figure S4. Studies on polymerization mechanism in traditional methods. (a) Normalized GPC-dRi trace of polymerization of Trp-NCA at room temperature in DMF without any catalysts. (b) Normalized GPC-LS traces of the obtained PLW at 25 ºC or 4 ºC. $[M]_0/[I]_0 = 50$, $[M]_0 = 0.2$ M.

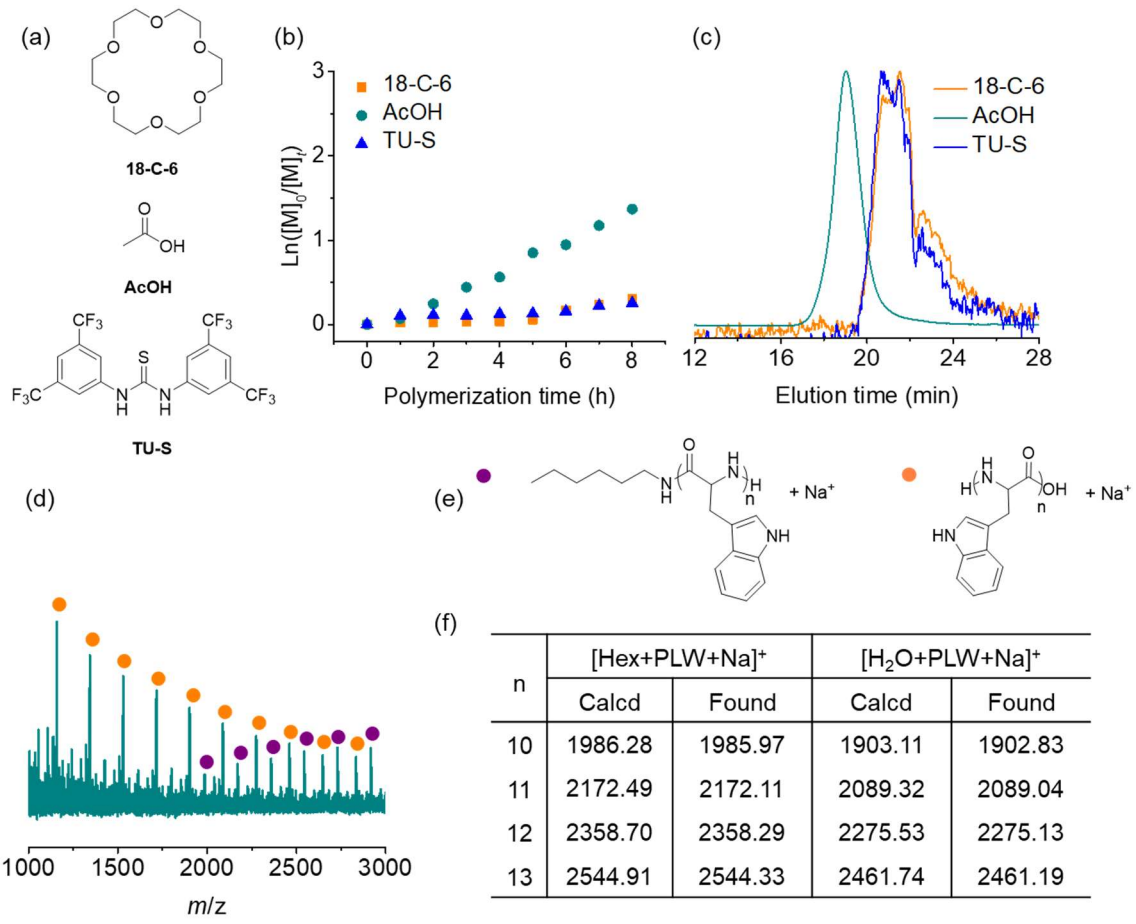

n	[Hex+PLW+Na]+		[H2O+PLW+Na]+	
	Calcd	Found	Calcd	Found
10	1986.28	1985.97	1903.11	1902.83
11	2172.49	2172.11	2089.32	2089.04
12	2358.70	2358.29	2275.53	2275.13
13	2544.91	2544.33	2461.74	2461.19

Figure S5. Comparison of the catalyzed ROP of Trp-NCA using different reported catalysts. (a) Chemical structures of various commercial catalysts. (b) Semilogarithmic kinetic plots of polymerization of Trp-NCA with different commercial catalysts. (c) Normalized GPC-LS traces of the obtained PLW catalyzed by different commercial catalysts. (d) MALDI-TOF characterization of resulting PLW from polymerization of Trp-NCA in the presence of AcOH. (e) Chemical structures of corresponding polymeric species in the MALDI-TOF MS analysis. (f) Comparison of representative *m*/z signals between calculated values from molecular formula and obtained values from MALDI-TOF spectra. $[M]_0/[I]_0$ = 50, $[M]_0$ = 0.2 M. $[I]_0/[Cat]_0$ = 1, 0.005, and 1 for the polymerization catalyzed by 18-C-6, AcOH, and TU-S, respectively.

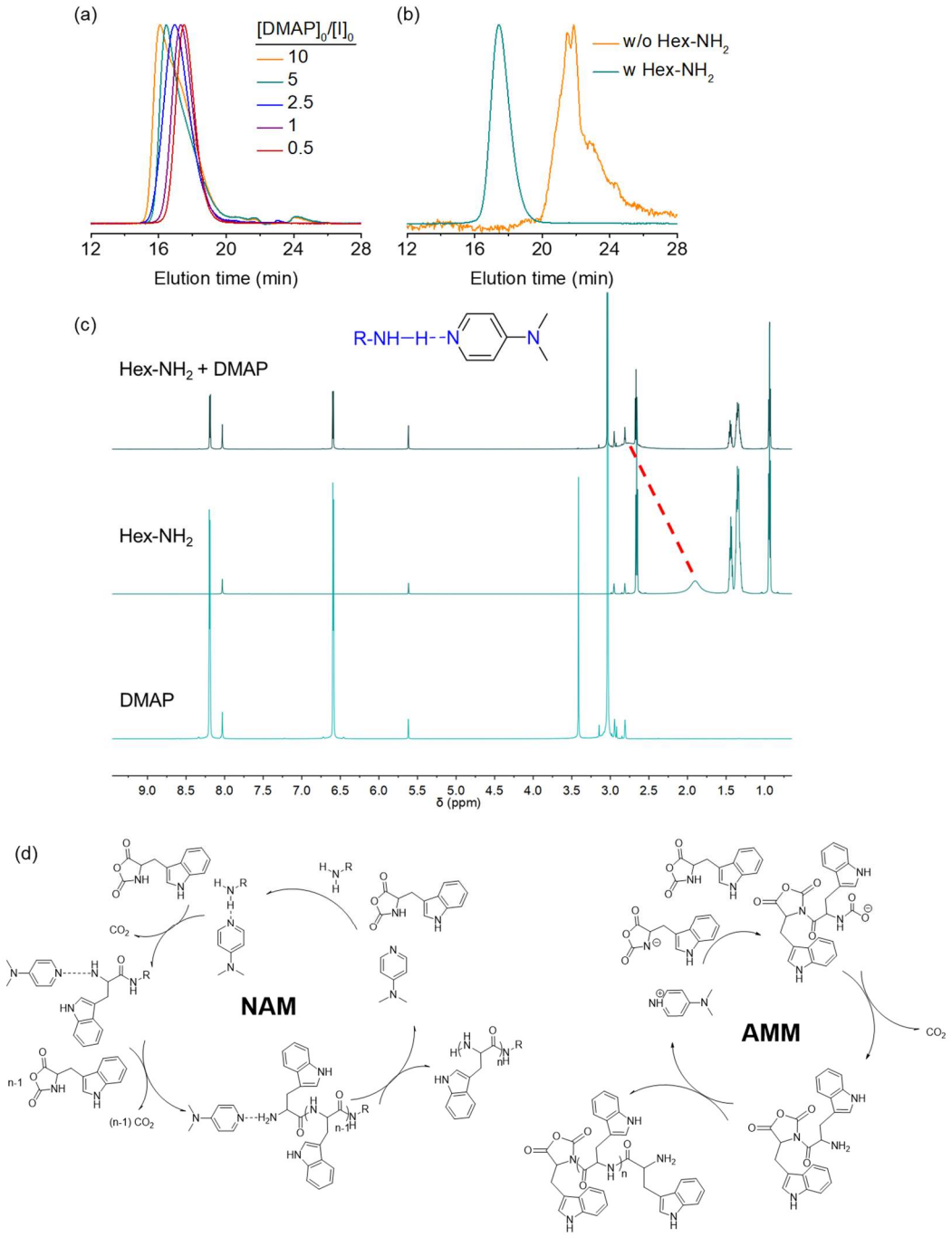

Figure S6. Studies on polymerization mechanism in the presence of DMAP. (a) Normalized GPC-LS traces of the resulting PLW with different $[DMAP]_0/[I]_0$ ratios. (b) Normalized GPC-LS traces of the resulting PLW in the presence or absence of Hex-NH_2 initiators at $[DMAP]_0/[I]_0$ = 1. $[M]_0$ = 0.2 M, $[M]_0/[I]_0$ = 50. (c) Interactions between DMAP and Hex-NH_2. $[Trp\text{-}NCA]_0/[Hex\text{-}NH_2]_0$ = 10 mM. (d) Possible reaction pathways for the NAM and AMM of Trp-NCA catalyzed or initiated by DMAP.

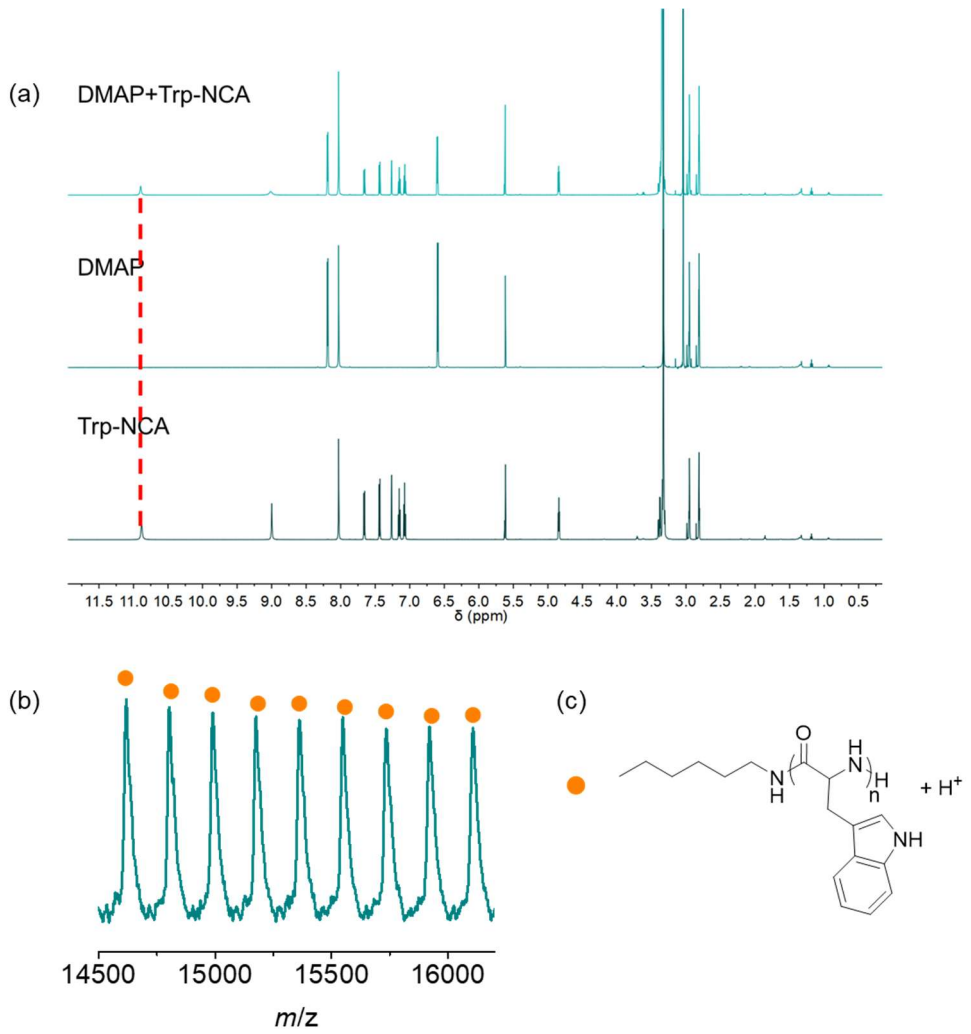

Figure S7. Studies on catalytic behavior of DMAP. (a) NMR titration of Trp-NCA upon addition of DMAP. $[\text{Trp-NCA}]_0/[\text{Hex-NH}_2]_0$ = 10 mM. (b) MALDI-TOF MS of the resulting PLW in the presence of DMAP. (e) Chemical structures of corresponding polymeric species in the MALDI-TOF MS analysis. The obtained *m*/*z* signals agreed well with the calculated values (101.19 + 186.21*n* + 1.01) corresponding to the polypeptides with *n*-hexyl tails.

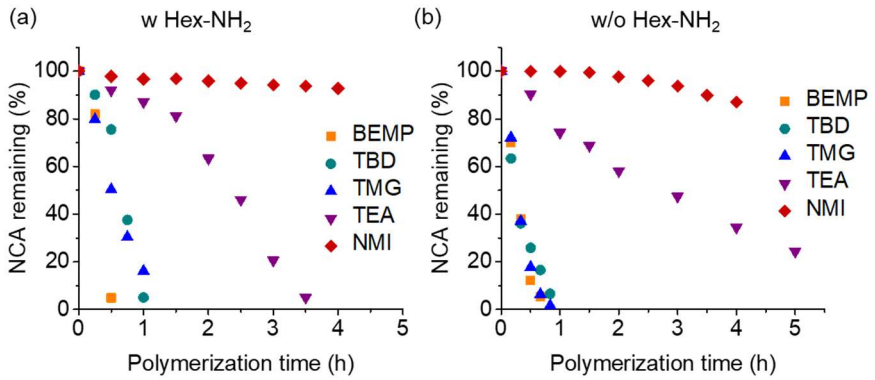

Figure S8. Comparison of ROP of Trp-NCA in the presence of various organic bases. Semilogarithmic kinetic plots of polymerization of Trp-NCA in the presence (a) or absence (b) of Hex-NH_2 with different organic base catalysts. $[M]_0/[I]_0$= 50, $[M]_0$ = 0.2 M.

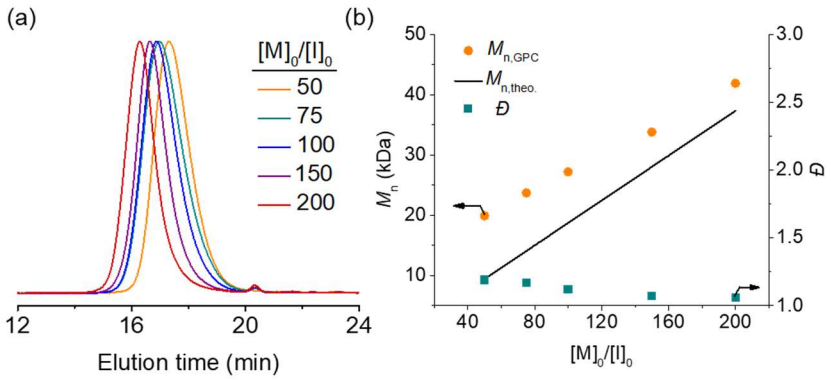

Figure S9. Characterization of resulting PLW from DMAP-catalyzed polymerization. (a) Normalized GPC-LS traces of the resulting PLW at various $[M]_0/[I]_0$ ratios. (b) MWs and dispersity of PLW at various $[M]_0/[I]_0$ ratios. $[M]_0$ = 0.2 M, $[DMAP]_0/[I]_0$ = 1.

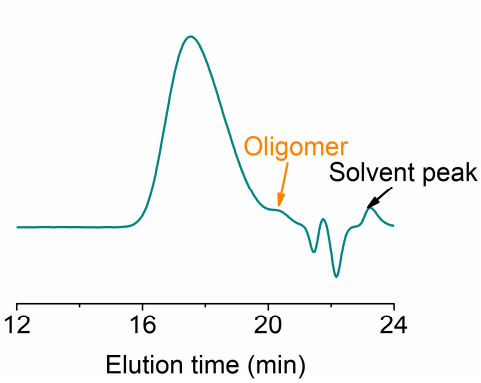

Figure S10. GPC-dRI trace of the resulting PLW from DMAP-catalyzed polymerization. $[M]_0/[I]_0 = 50$, $[M]_0 = 0.2$ M, $[DMAP]_0/[I]_0 = 1$.

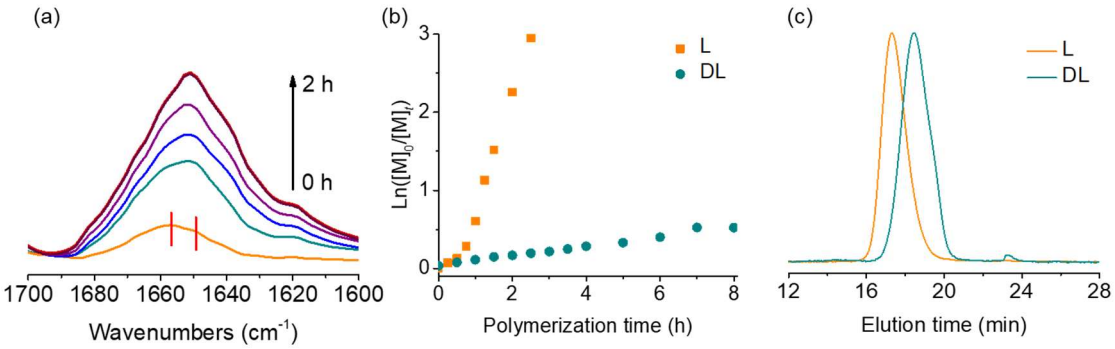

Figure S11. Two-stage kinetics of DMAP-catalyzed polymerization of Trp-NCA. (a) Overlaid FTIR spectra monitoring the DMAP-catalyzed polymerization of Trp-NCA. The highlighted peaks (1649 and 1655 cm^{-1}) suggested the formation of α-helical and random-coiled conformations (amide I) at the early stages of the polymerization. (b) Semilogarithmic kinetic plots of polymerization of Trp-NCA and its racemic DL-tryptophan NCA analogue. (c) Normalized GPC-LS traces of the resulting polypeptides. $[M]_0/[I]_0 = 50$, $[M]_0 = 0.2$ M, $[DMAP]_0/[I]_0 = 1$.

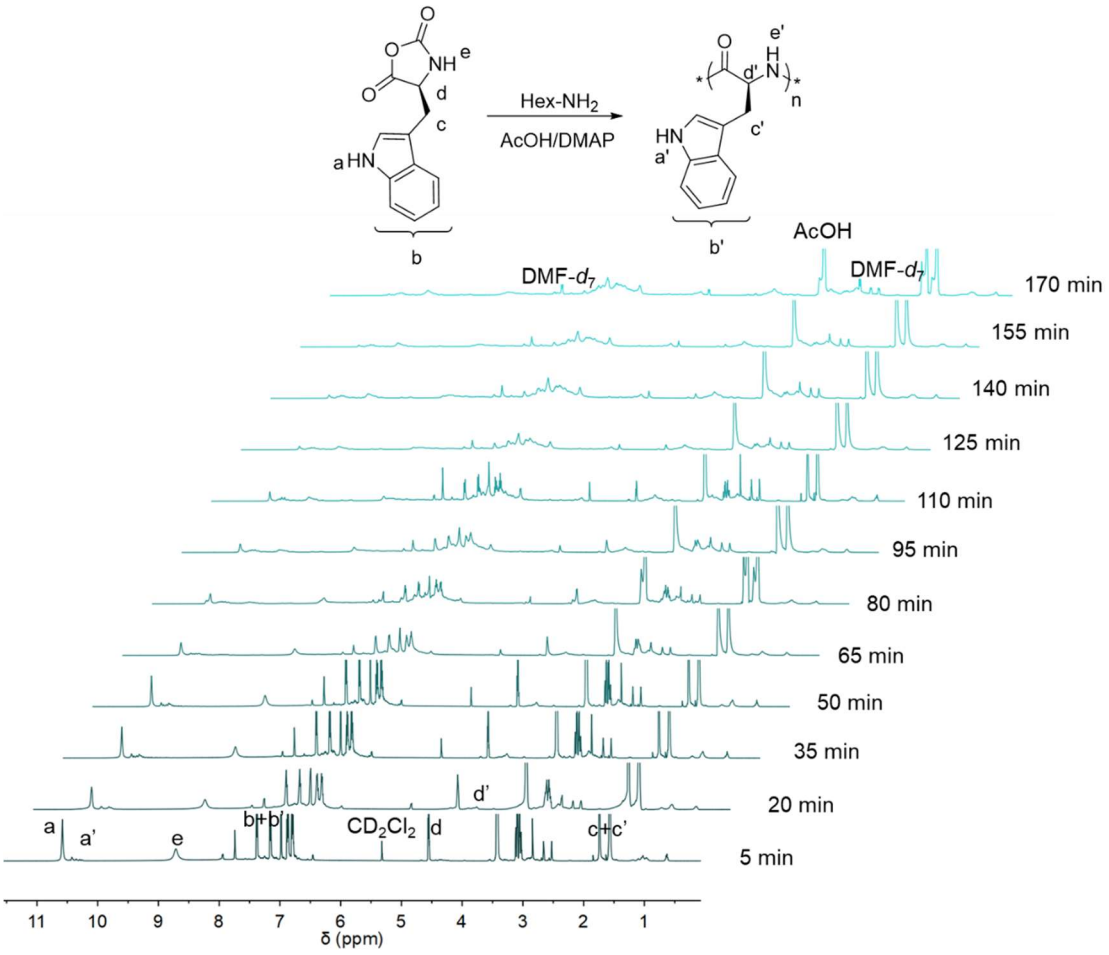

Figure S12. Overlaid NMR spectra (600 MHz) showing the polymerization process in the presence of AcOH/DMAP in DMF-d_7/CD_2Cl_2. $[M]_0/[I]_0$ = 50, $[M]_0$ = 0.2 M, $[DMAP]_0/[I]_0$= 1, $[M]_0/[AcOH]_0$ = 1.

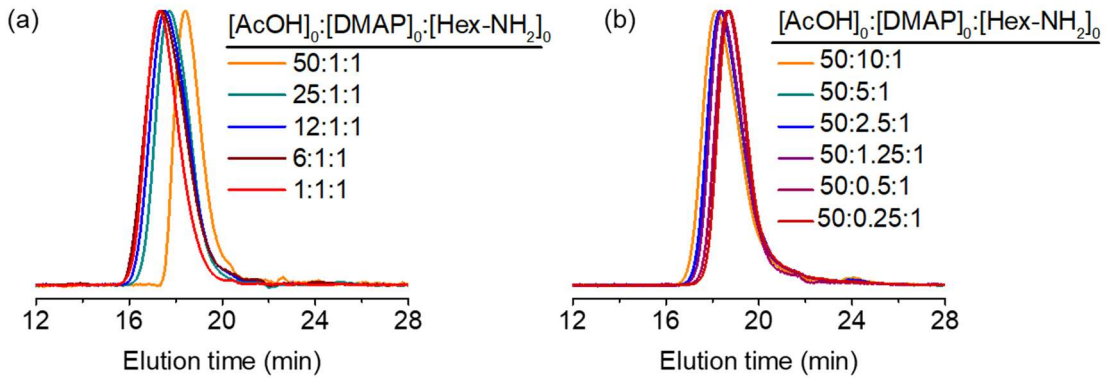

Figure S13. Normalized GPC-LS traces of the resulting PLW from polymerization of Trp-NCA under different AcOH/DMAP ratios. (a) AcOH amount was varied while the DMAP and initiator loadings were kept constant. (b) DMAP amount was varied while the AcOH and monomer loadings were kept constant. $[M]_0/[I]_0 = 50$, $[M]_0 = 0.2$ M.

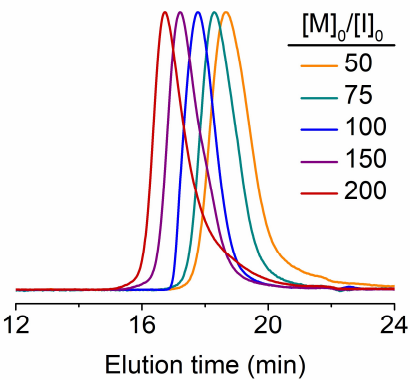

Figure S14. Normalized GPC-LS traces of the resulting PLW from polymerization of Trp-NCA in the presence of AcOH/DMAP at various $[M]_0/[I]_0$ ratios. $[M]_0$ = 0.2 M, $[DMAP]_0/[I]_0$ = 1, $[M]_0/[AcOH]_0$ = 1.

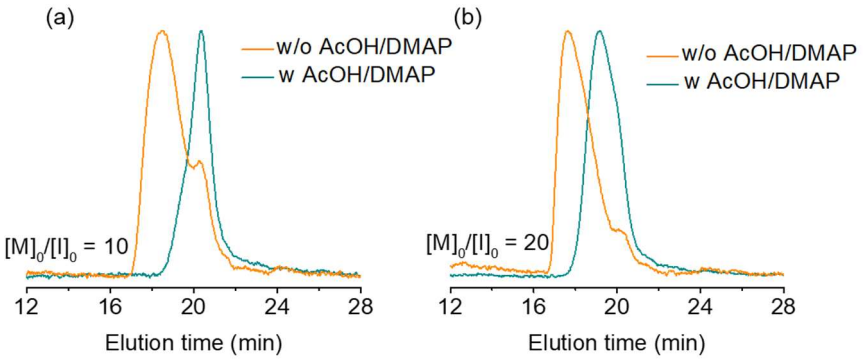

Figure S15. Normalized GPC-LS traces of obtained oligo(L-tryptophan) at $[M]_0/[I]_0$ values of 10 (a) and 20 (b) in the presence or absence of AcOH/DMAP. $[M]_0$ = 0.2 M, $[DMAP]_0/[I]_0$ = 1, $[M]_0/[AcOH]_0$ = 1.

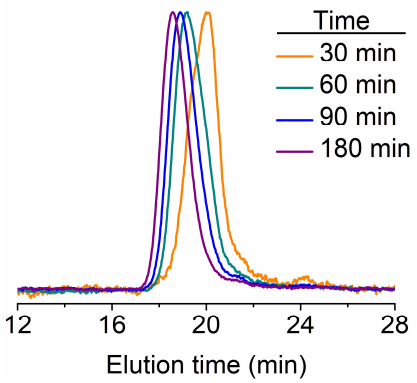

Figure S16. Normalized GPC-LS traces of PLW from polymerization of Trp-NCA in the presence of AcOH/DMAP at various monomer conversions. $[M]_0/[I]_0 = 50$, $[M]_0 = 0.2$ M, $[DMAP]_0/[I]_0 = 1$, $[M]_0/[AcOH]_0 = 1$.

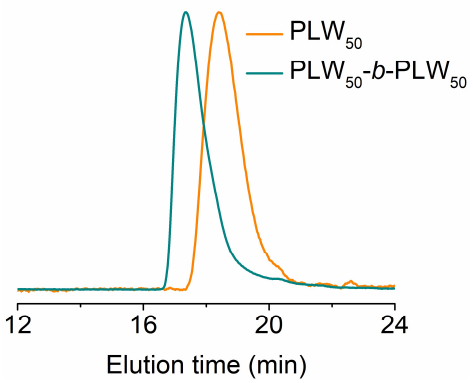

Figure S17. Normalized GPC-LS traces of diblock PLW-*b*-PLW and its first-block intermediate synthesized from the polymerization in the presence of AcOH/DMAP. $[M]_0/[I]_0 = 50$, $[M]_0 = 0.2$ M, $[DMAP]_0/[I]_0 = 1$, $[M]_0/[AcOH]_0 = 1$.

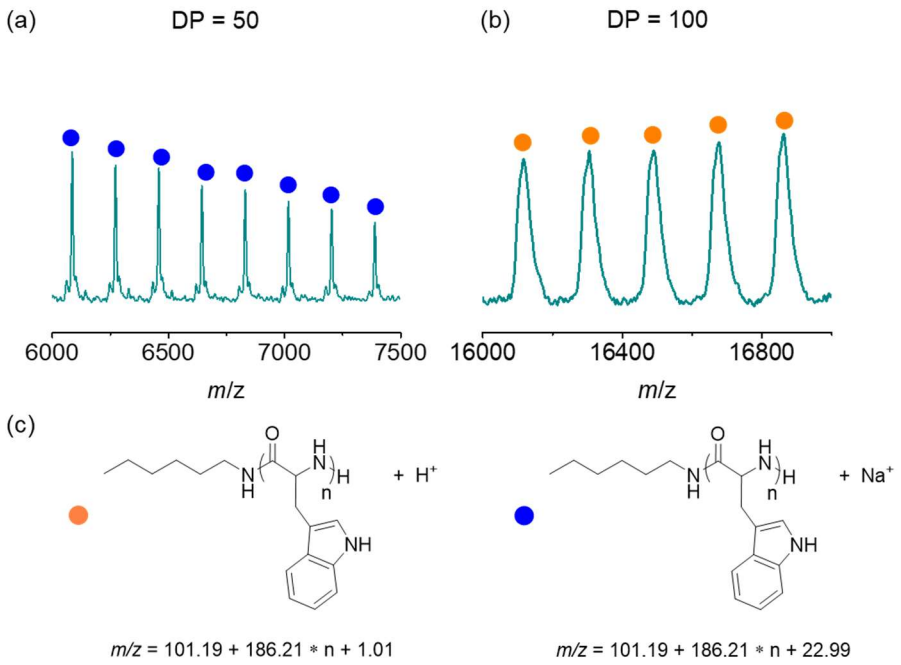

(d)

n	[Hex+PLW+Na]+	
	Calcd	Found
32	6078.10	6078.86
33	6264.16	6265.19
34	6450.22	6450.94
35	6636.28	6636.26
36	6822.34	6822.62
37	7008.40	7008.91

(e)

n	[Hex+PLW+H]+	
	Calcd	Found
86	16116.26	16117.03
87	16302.47	16303.81
88	16488.68	16489.32
89	16674.89	16675.54
90	16861.10	16862.36

Figure S18. MALDI-TOF characterization of resulting PLW from polymerization of Trp-NCA in the presence of AcOH/DMAP. (a, b) MALDI-TOF MS spectra of resulting PLW with $[M]_0/[I]_0$ value of 50 (a) and 100 (b). (c) Chemical structures of corresponding polymeric species in the MALDI-TOF MS analysis. (d-e) Comparison of representative *m*/z signals between calculated values from molecular formula and obtained values from MALDI-TOF spectra in (a-c). $[M]_0$ = 0.2 M, $[DMAP]_0/[I]_0$ = 1, $[M]_0/[AcOH]_0$ = 1.

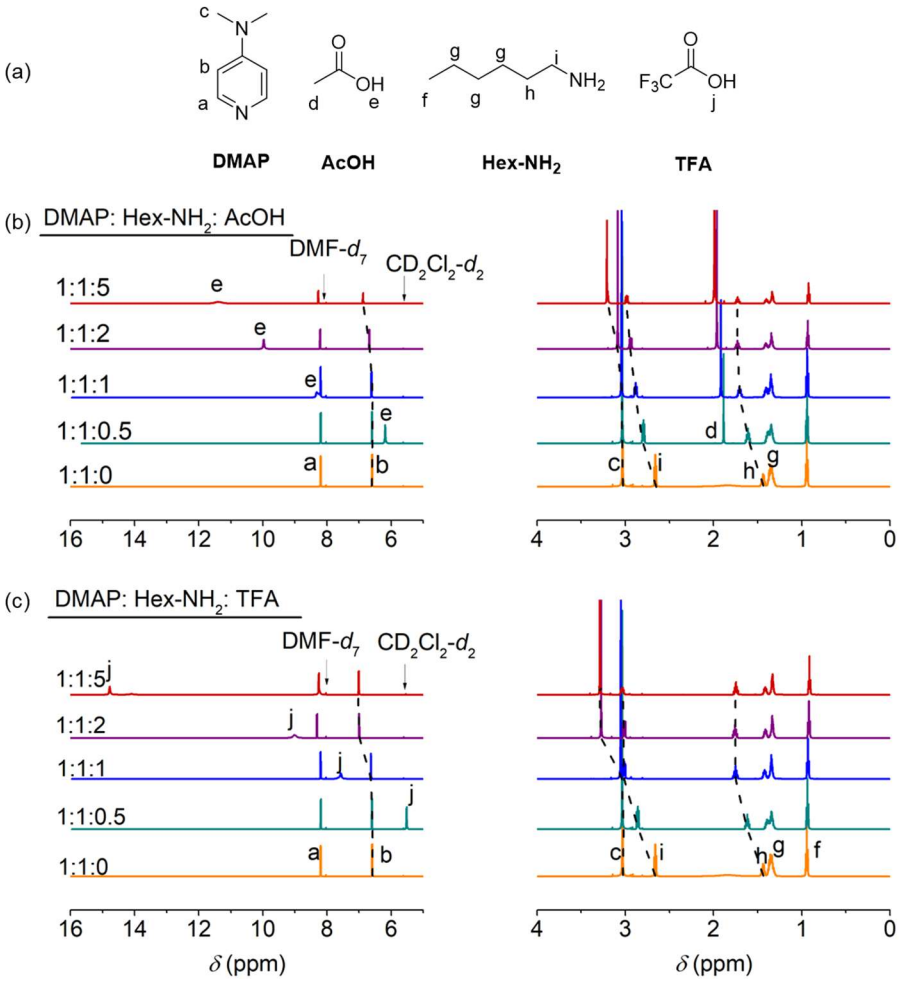

Figure S19. Quantification of ionization fraction of DMAP and Hex-NH_2 through NMR titration. (a) Chemical structures of DMAP, AcOH, Hex-NH_2, and TFA. (b, c) Overlaid ^{1}H NMR spectra of the mixture of DMAP and Hex-NH_2 with AcOH (b) and TFA (c) in DMF-d_7/CD_2Cl_2 at various $[acid]_0/[Hex\text{-}NH_2]_0$ ratios. $[Hex\text{-}NH_2]_0$ = 0.2 M. The protons with significant changes in chemical shift was highlighted with black dashed lines.

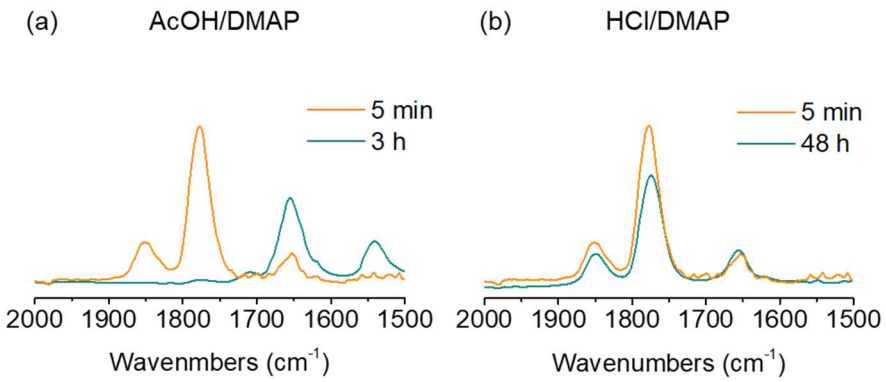

Figure S20. Effect of acid on polymerization behavior. Overlaid FTIR spectra showing the polymerization of Trp-NCA in the presence of AcOH/DMAP (a) or HCl/DMAP (b) in DMF/DCM. $[M]_0/[I]_0 = 50$, $[M]_0 = 0.2$ M, $[DMAP]_0/[I]_0 = 1$, $[M]_0/[AcOH]_0 = 1$.

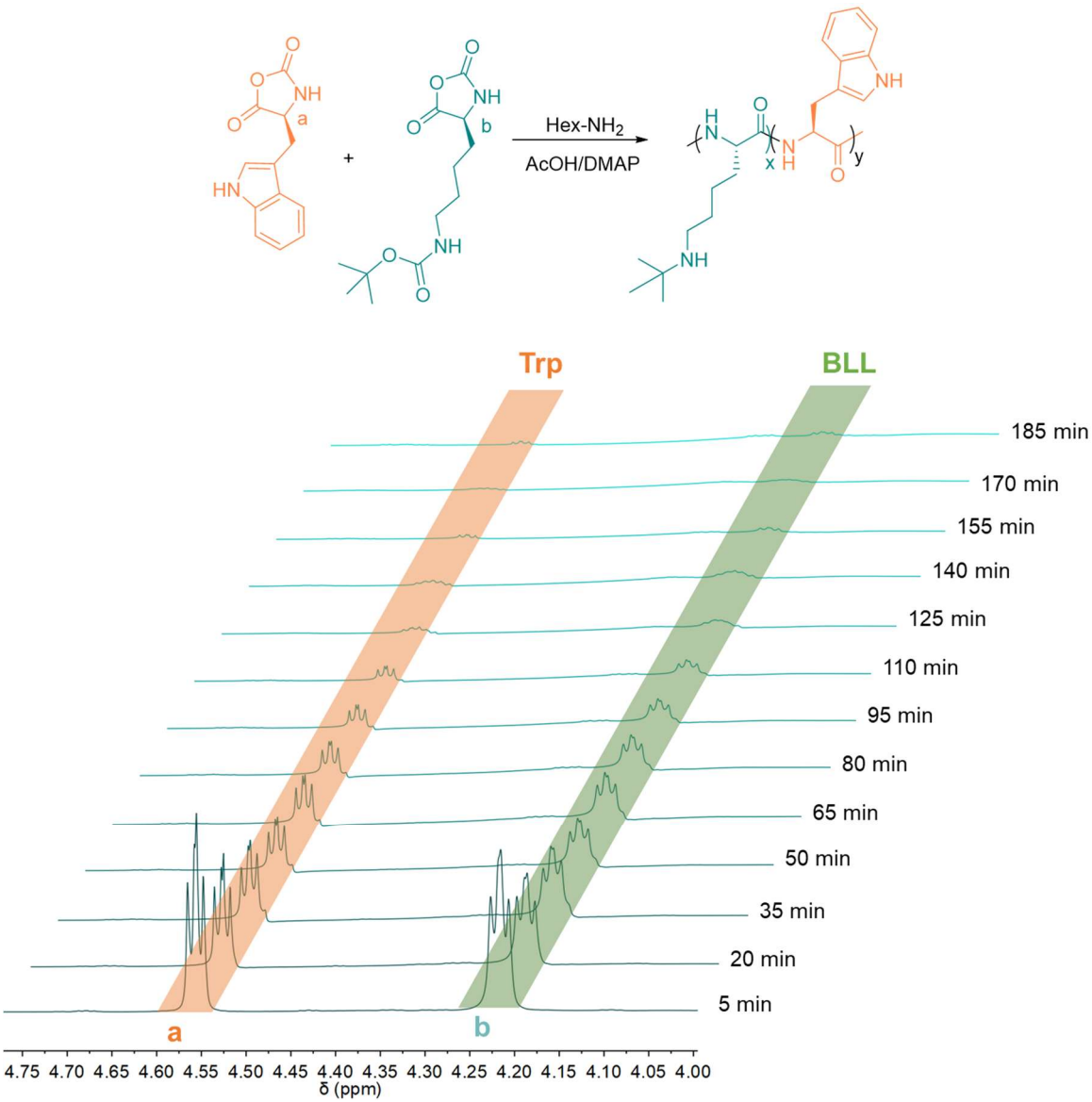

Figure S21. Time-resolved ^{1}H NMR spectra (600 MHz) showing the copolymerization of Trp-NCA and BLL-NCA in DMF-d_7/CD_2Cl_2. $[M]_0/[I]_0$ = 100, $[M]_0$ = 0.2 M, $[DMAP]_0/[I]_0$ = 1, $[M]_0/[AcOH]_0$ = 1, $[Trp\text{-}NCA]_0/[BLL\text{-}NCA]_0$ = 1.

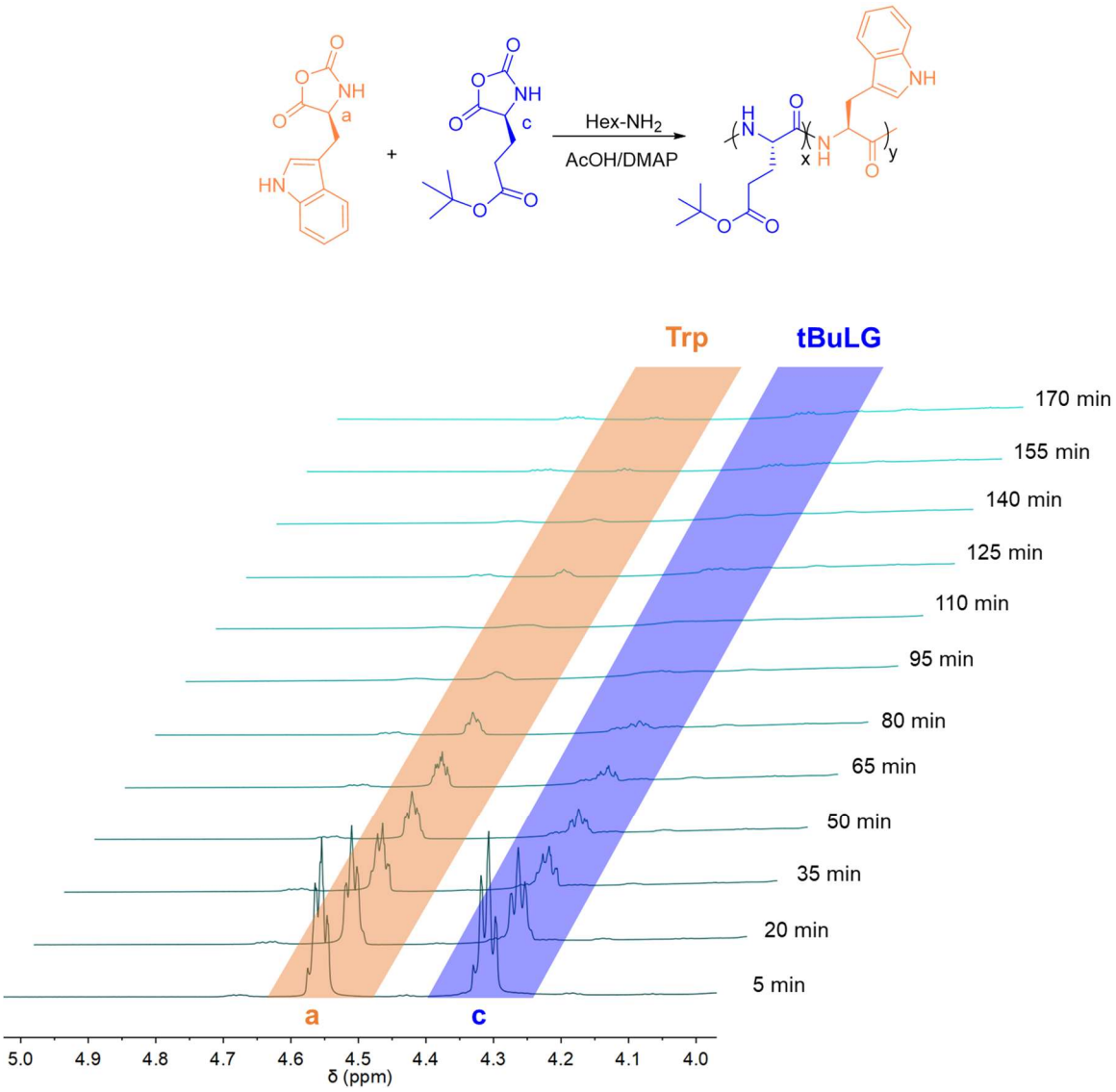

Figure S22. Time-resolved ^{1}H NMR spectra (600 MHz) showing the copolymerization of Trp-NCA and BLL-NCA in DMF-d_7/CD_2Cl_2. $[M]_0/[I]_0$ = 100, $[M]_0$ = 0.2 M, $[DMAP]_0/[I]_0$ = 1, $[M]_0/[AcOH]_0$ = 1, $[Trp\text{-}NCA]_0/[tBuLG\text{-}NCA]_0$ = 1.

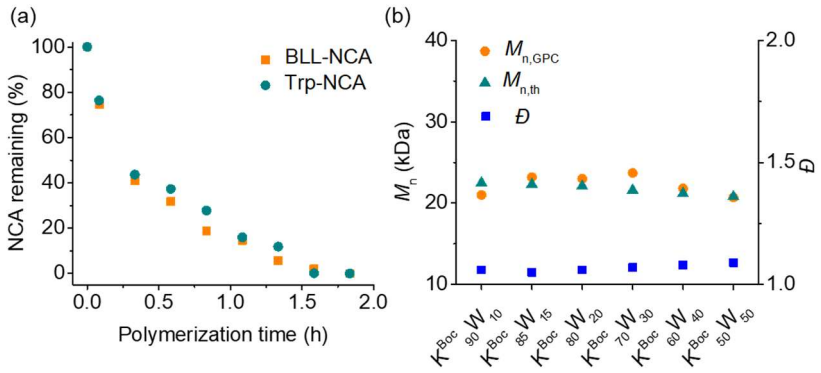

Figure S23. The copolymerization behavior of BLL-NCA and Trp-NCA. (a) Semilogarithmic kinetic plot of copolymerization of BLL-NCA and Trp-NCA in the presence AcOH/DMAP. (b) MWs and dispersity of K^{Boc}-*co*-W obtained from copolymerization of Trp-NCA and BLL-NCA mixtures. $[M]_0/[I]_0 = 100$, $[M]_0 = 0.2$ M, $[DMAP]_0/[I]_0 = 1$, $[M]_0/[AcOH]_0 = 1$.

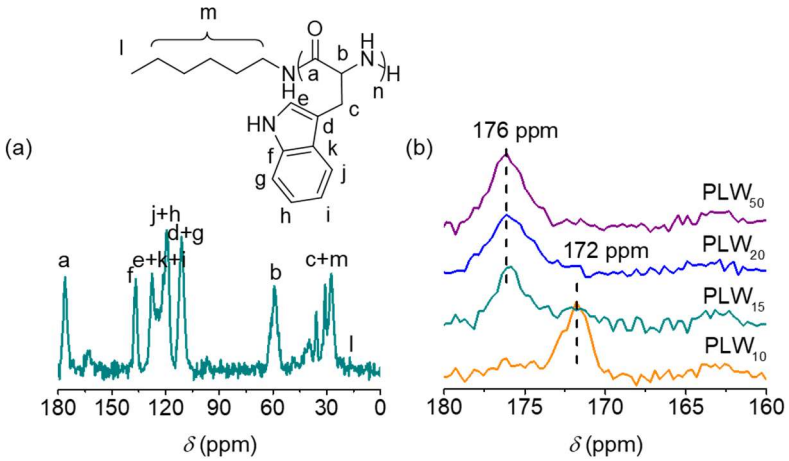

Figure S24. Representative ^{13}C CP/MAS NMR spectra of PLW_{50} (a) and expanded spectra of the backbone carboxyl region of PLW with different DP (b).

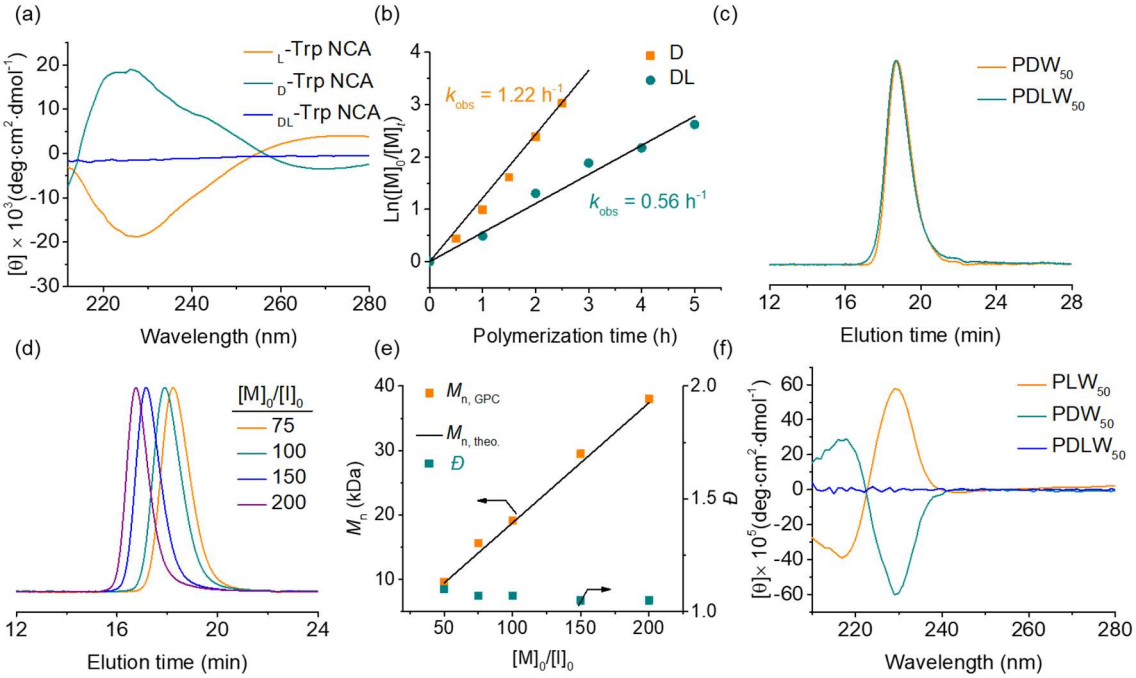

Fig S25. Polymerization behavior and chiroptical properties of monomers with different chiral configurations. (a) CD spectra of L, D and DL monomers (b) Semilogarithmic kinetic plot of polymerization of D and DL monomers in the presence AcOH/DMAP. (c) Normalized GPC-LS traces of PDW_{50} and $PDLW_{50}$. (d) Normalized GPC-LS traces of the resulting PDW from polymerization of Trp-NCA in the presence of AcOH/DMAP at various $[M]_0/[I]_0$ ratios. (e) M_n-conversion plot of the polymerization of D-Trp NCA in the presence of AcOH/DMAP. (f) CD spectra of PLW_{50}, PDW_{50}, and $PDLW_{50}$. $[M]_0$ = 0.2 M, $[DMAP]_0/[I]_0$ = 1, $[M]_0/[AcOH]_0$ = 1.

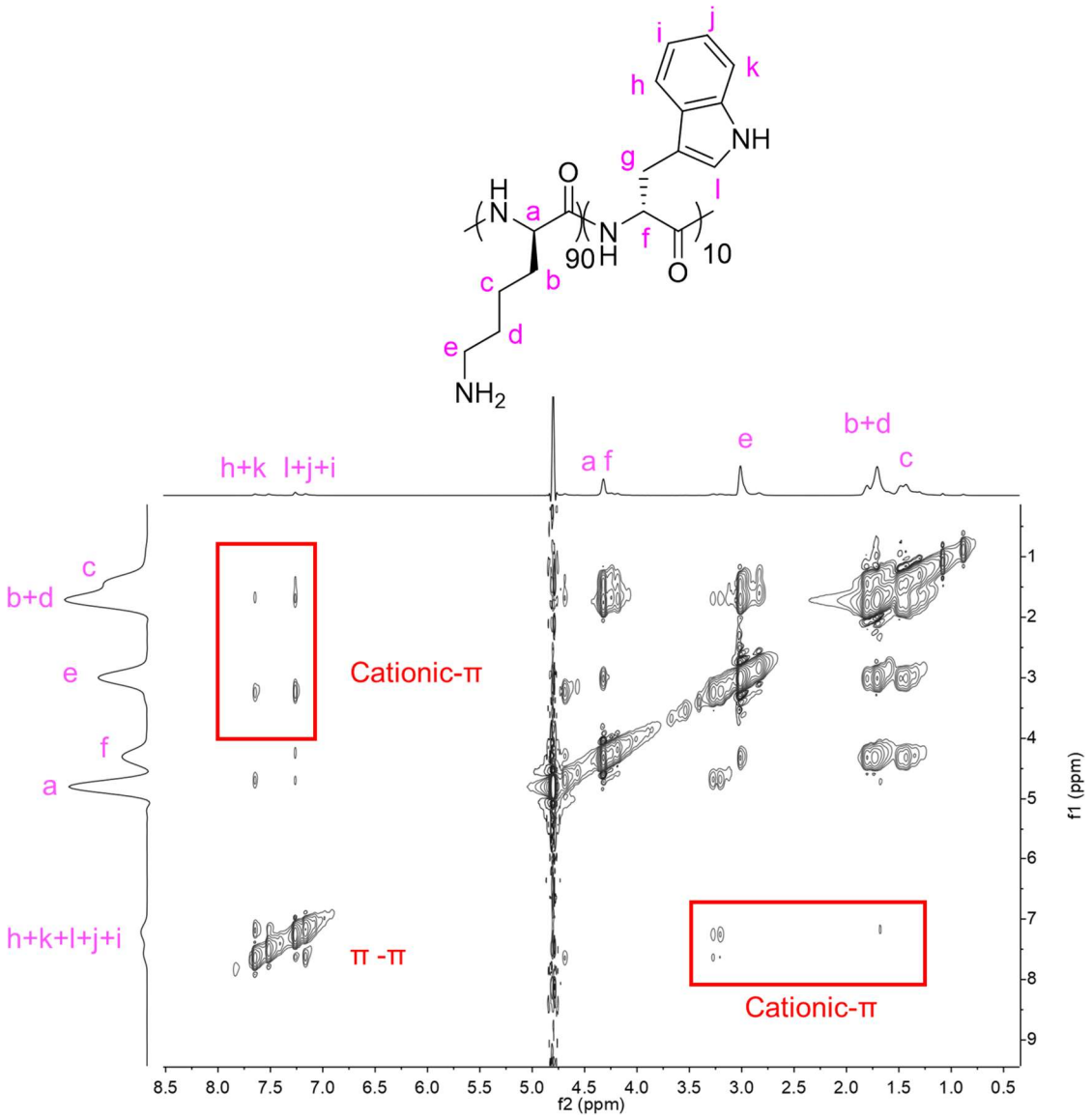

Figure S26. 2D NOESY spectra of $K_{90}W_{10}$ in D_2O. Distinct NOE signals are observed in $K_{90}W_{10}$, specifically between the indole ring $H_{h\text{-}k}$ of tryptophan and the side chain $H_{a\text{-}e}$ of lysine.

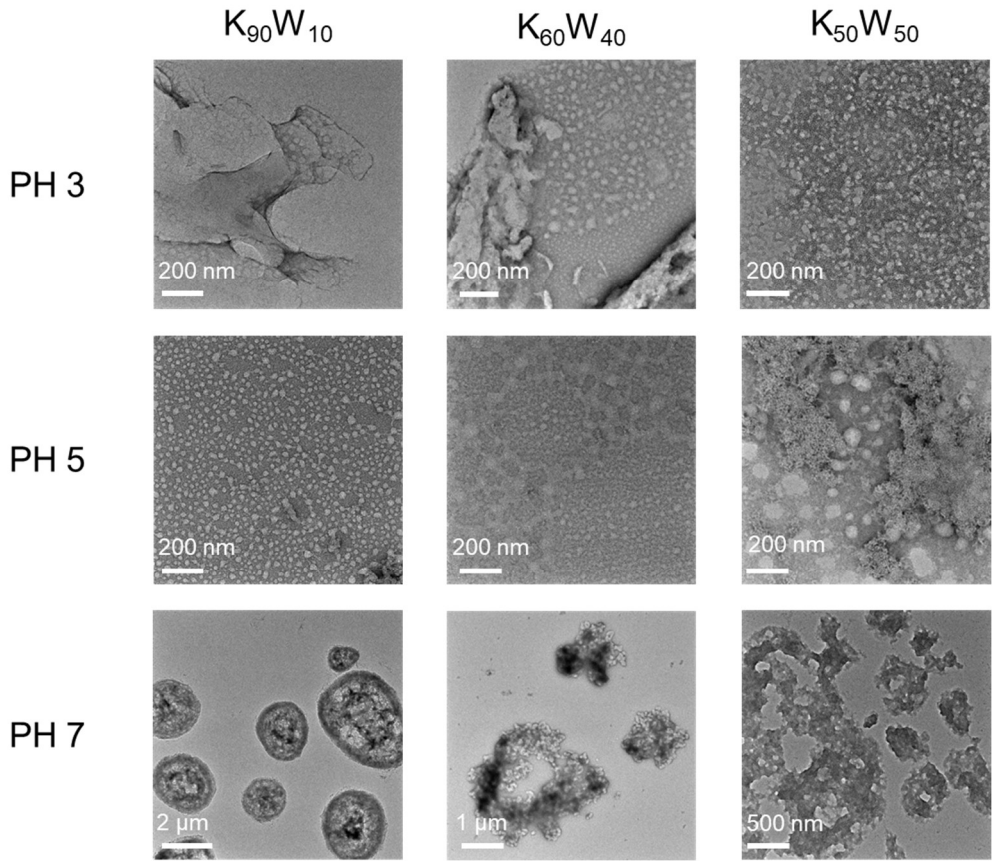

Figure S27. Representative HRTEM images of the different copolymer nanoparticles obtained with $K_{90}W_{10}$, $K_{60}W_{40}$ and $K_{50}W_{50}$ in disodium hydrogen phosphate/citric acid buffer solutions at different pH values.

NMR Spectra and Single Crystal Diffraction Data

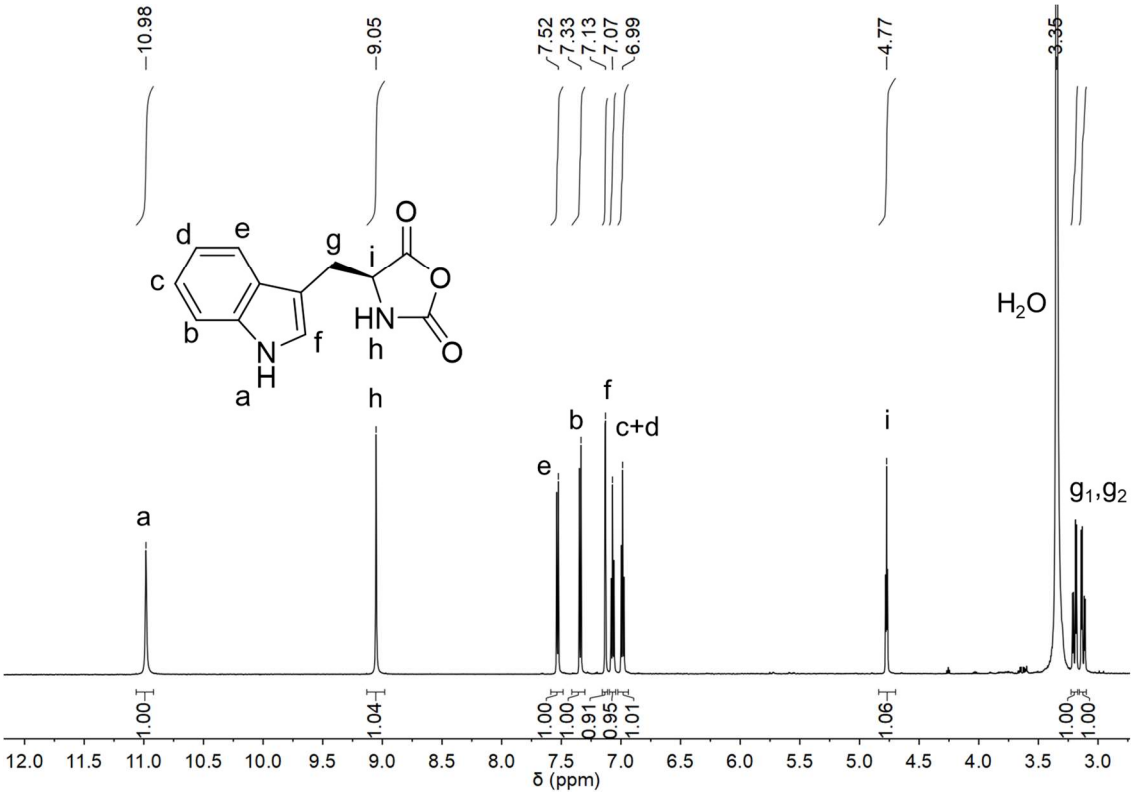

Figure S28. ^{1}H NMR spectrum (600 MHz) of Trp-NCA in DMSO-d_6.

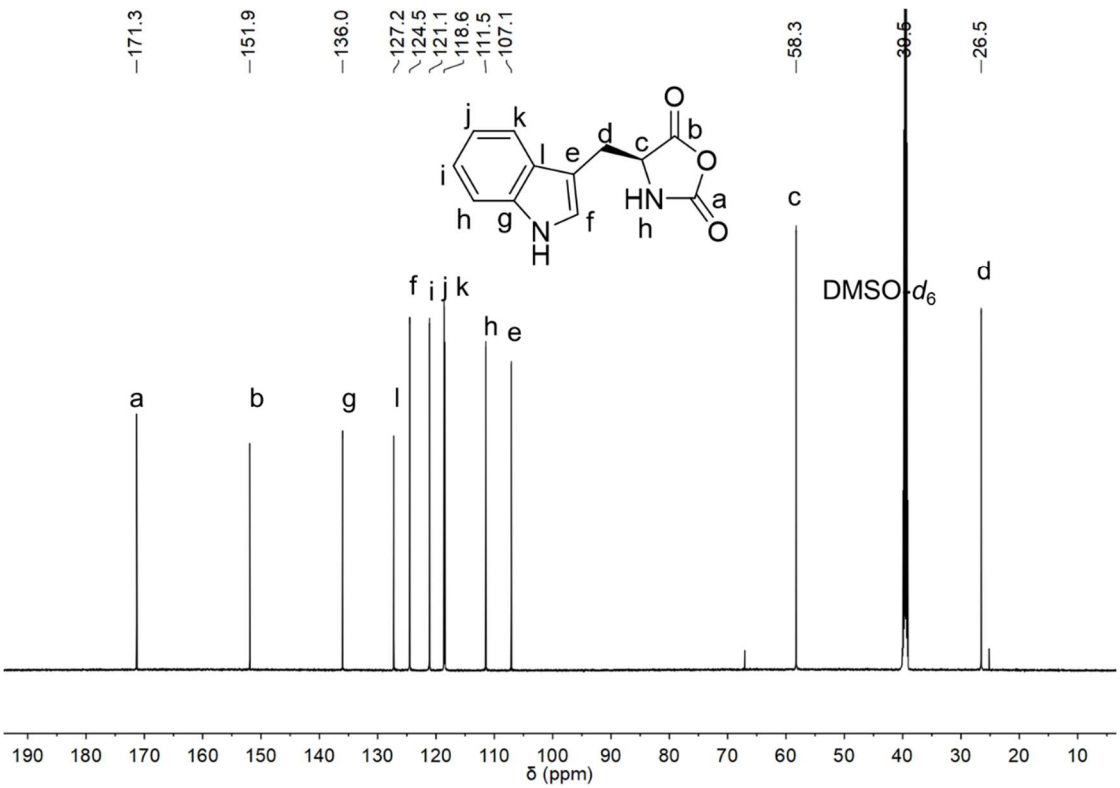

Figure S29. ^{13}C NMR spectrum (151 MHz) of Trp-NCA in DMSO-d_6.

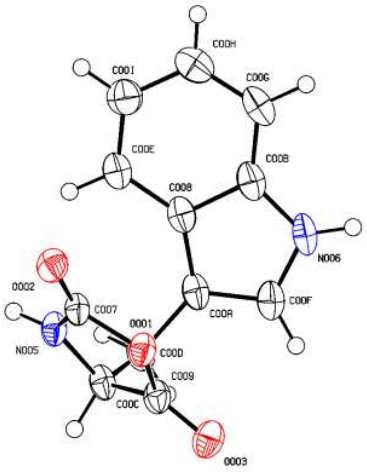

Figure S30. Structure of Trp-NCA by single-crystal X-ray diffraction.

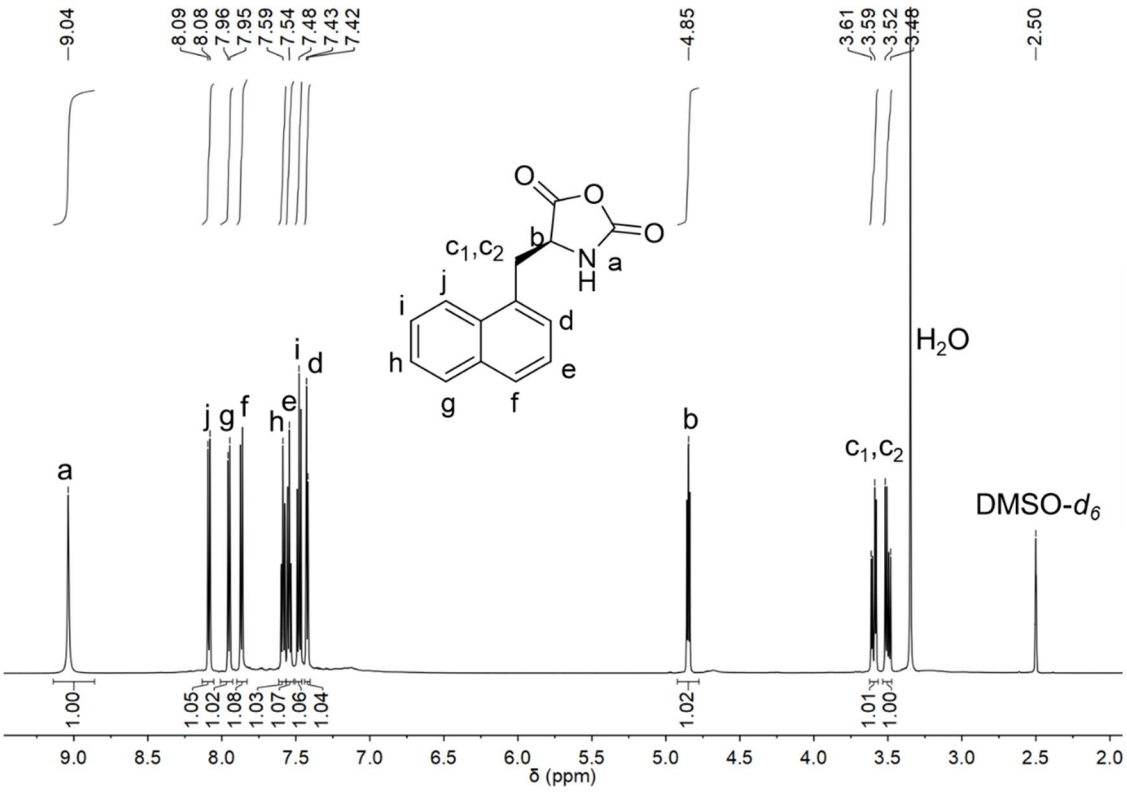

Figure S31. ^{1}H NMR spectrum (600MHz) of Nap-NCA in DMSO-d_6.

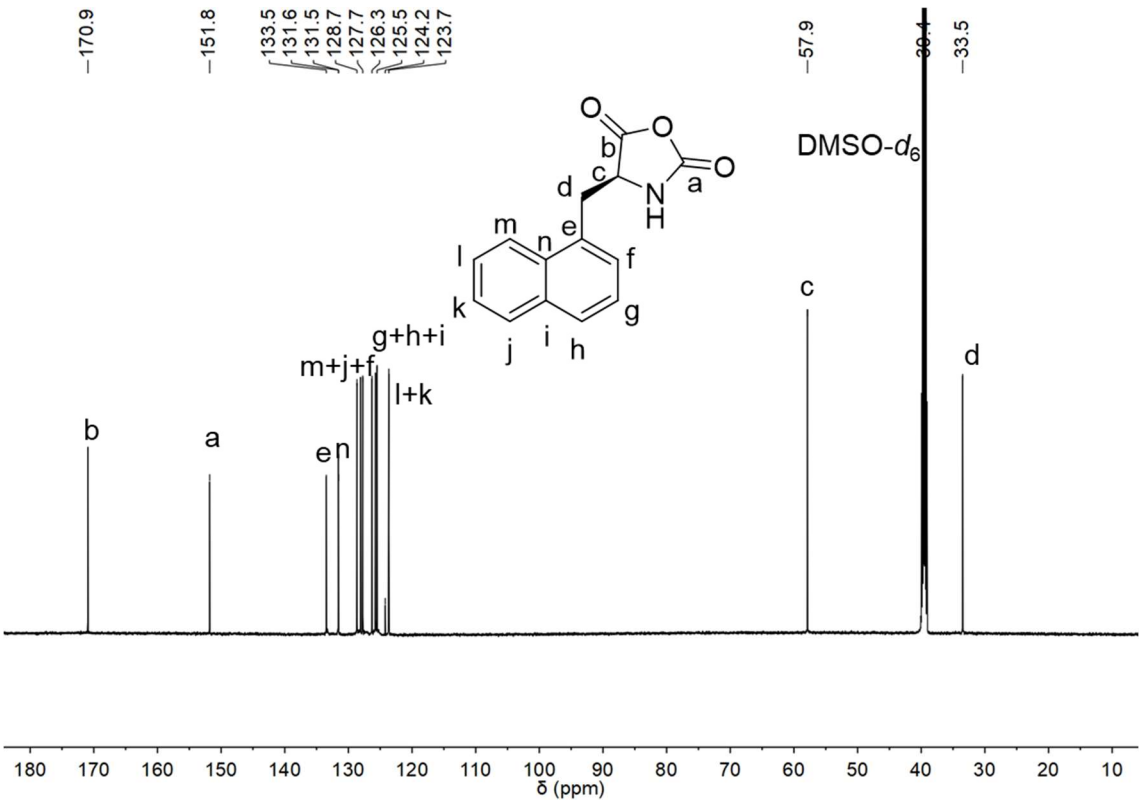

Figure S32. ^{13}C NMR spectrum (151 MHz) of 1-Nap-NCA in DMSO-d_6.

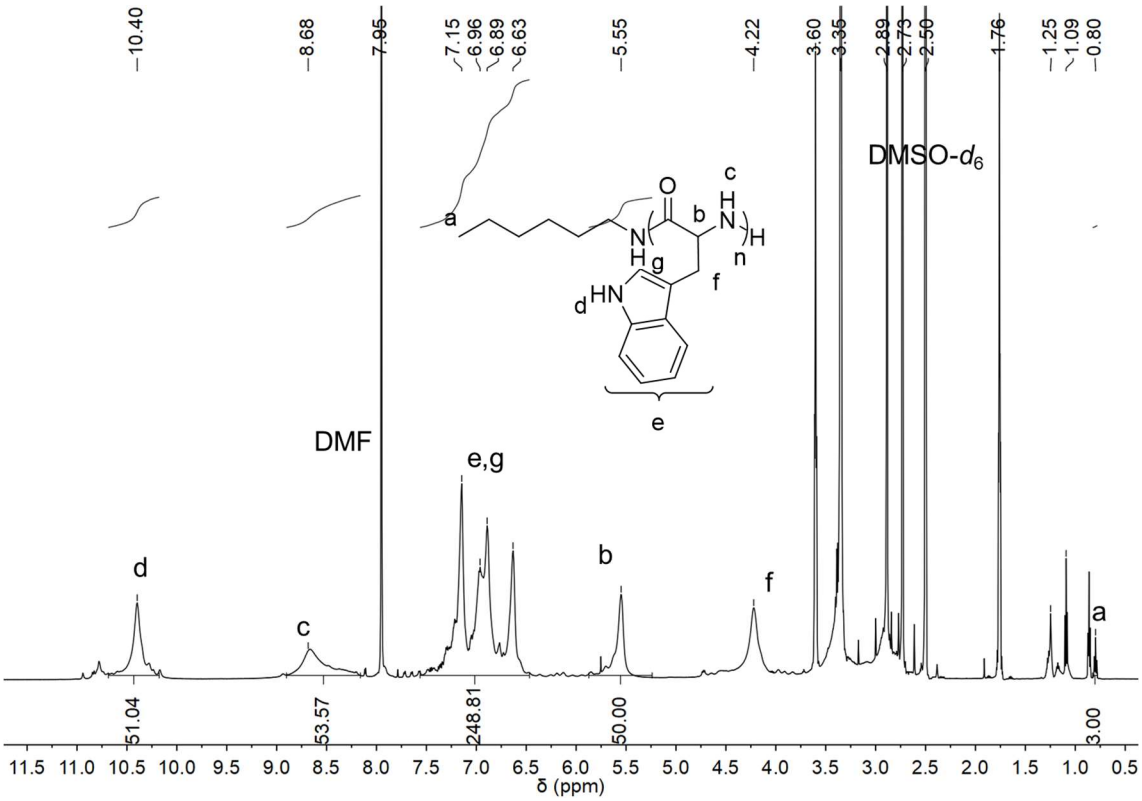

Figure S33. ^{1}H NMR spectrum (600 MHz) of PLW_{50} in DMSO-d_6.

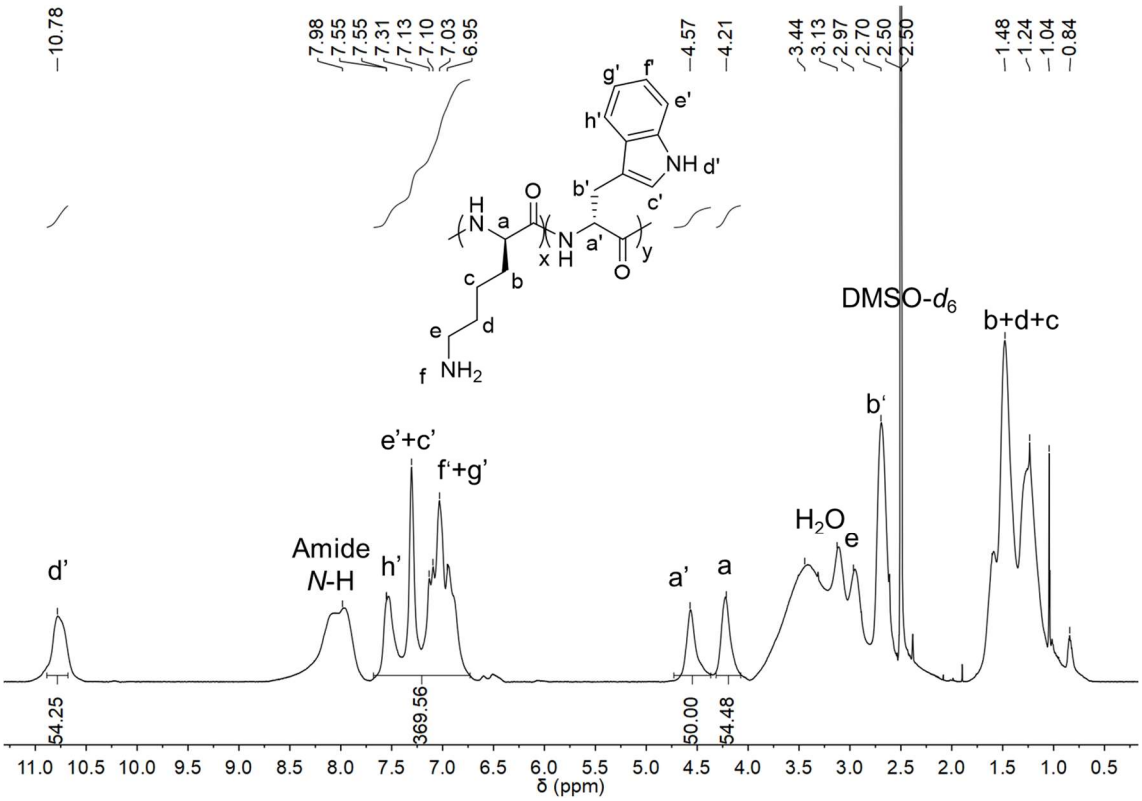

Figure S34. ^{1}H NMR spectrum (600 MHz) of $K_{50}W_{50}$ in DMSO-*d*$_6$.

Supporting Tables

Table S1. Characterization of resulting polypeptides from polymerization of Trp-NCA at different temperatures.[a]

Entry	T (ºC)	t (h)[b]	$M_{n,\,GPC}$ (kDa)[c]	$Đ$[c]
1	25	48	19.9	1.19
2	4	72	12.6	1.05

[a]Both polymerizations were conducted at room temperature in DMF/DCM (1:1, v/v) with Hex-NH_2 as the initiator and Trp-NCA as the monomer. $[M]_0/[I]_0 = 50$, $[M]_0 = 0.2$ M. The theoretical MW was 9.4 kDa. [b]Polymerization time reaching 95% monomer conversion. [c]Determined by GPC; dn/dc = 0.125.

Table S2. Characterization of resulting polypeptides from polymerization of Trp-NCAs in different catalytic systems.[a]

Entry	Catalyst	$M_{n,\,GPC}$ (kDa)[b]	$Đ$[b]
1	18-crown-6	5.6	1.11
2	AcOH	11.4	1.08
3	TU-S	5.0	1.08

[a]All polymerizations were conducted at room temperature in DMF/DCM (1:1, v/v) with Hex-NH_2 as the initiator and Trp-NCA as the monomer. $[M]_0/[I]_0 = 50$, $[M]_0 = 0.2$ M. $[I]_0/[Cat]_0 = 1$, 0.005, and 1 for the polymerization catalyzed by 18-C-6, AcOH, and TU-S, respectively. [b]Polymerization time reaching 95% monomer conversion. [c]Determined by GPC; dn/dc = 0.125.

Table S3. Polymerization of Trp-NCA in the presence of DMAP.[a]

Entry	$[M]_0/[I]_0$	t (h)[b]	$M_{n,theo.}$ (kDa)	$M_{n,GPC}$ (kDa)[c]	$Đ$[c]
1	75	3	14.1	23.7	1.17
2	100	4	18.7	27.2	1.12
3	150	6	28.0	33.8	1.07
4	200	8	37.3	41.9	1.06
5[d]	50	48	9.41	10.3	1.20

[a]All polymerizations were conducted at room temperature in DCM/DMF cosolvents (1:1, v/v) with Hex-NH_2 as the initiator, Trp-NCA as the monomer, and DMAP as the catalyst. $[M]_0$ = 0.2 M, $[DMAP]_0/[I]_0$ = 1. The monomers conversions were > 95% for all polymerizations as determined by FTIR. [b]Polymerization time reaching 95% monomer conversion. [c]Determined by GPC. dn/dc = 0.125. [d]$_{DL}$-tryptophan NCA was used as monomer.

Table S4. Polymerization of Trp-NCA under different AcOH/DMAP ratios at fixed DMAP amount.[a]

Entry	$[AcOH]_0/[DMAP]_0$	t (h)[b]	$M_{n,theo.}$ (kDa)	$M_{n,GPC}$ (kDa)[c]	$Đ$[c]
1	50	3	9.4	11.1	1.05
2	25	3	9.4	17.0	1.13
3	12.5	3	9.4	18.0	1.15
4	6.25	3	9.4	19.6	1.16
5	1	3	9.4	21.3	1.15

[a]All polymerizations were conducted at room temperature in DCM/DMF cosolvents (1:1, v/v) with Hex-NH_2 as the initiator, Trp-NCA as the monomer, and AcOH/DMAP as the catalyst. $[M]_0$ = 0.2 M, $[DMAP]_0/[I]_0$ = 1. The monomers conversions were > 95% for all polymerizations as determined by FTIR. [b]Polymerization time reaching 95% monomer conversion. [c]Determined by GPC. dn/dc = 0.125.

Table S5. Polymerization of Trp-NCA under different AcOH/DMAP ratios at fixed AcOH amount.[a]

Entry	$[DMAP]_0/[I]_0$	t (h)[b]	$M_{n,theo.}$ (kDa)	$M_{n,GPC}$ (kDa)[c]	$Đ$[c]
1	10	1	9.4	11.3	1.20
2	5	1	9.4	10.6	1.15
3	2.5	1.5	9.4	10.7	1.16
4	1.25	3	9.4	11.7	1.09
5	0.5	6	9.4	10.9	1.05
6	0.25	15	9.4	10.6	1.05

[a]All polymerizations were conducted at room temperature in DCM/DMF cosolvents (1:1, v/v) with Hex-NH_2 as the initiator, Trp-NCA as the monomer, and AcOH/DMAP as the catalyst. $[M]_0$ = 0.2 M, $[M]_0/[AcOH]_0$ = 1. The monomers conversions were > 95% for all polymerizations as determined by FTIR. [b]Polymerization time reaching 95% monomer conversion. [c]Determined by GPC. dn/dc = 0.125.

Table S6. Polymerization of Trp-NCA at low $[M]_0/[I]_0$ in the presence of AcOH/DMAP.[a]

Entry	Additive	$[M]_0/[I]_0$	$M_{n,theo.}$ (kDa)	$M_{n,GPC}$ (kDa)[c]	$Đ$[c]
1	-	10:1	2.0	4.7	1.63
2	-	20:1	3.8	7.2	1.73
3	AcOH/DMAP	10:1	2.0	2.0	1.05
4	AcOH/DMAP	20:1	3.8	4.2	1.09

[a]All polymerizations were conducted at room temperature in DCM/DMF cosolvents (1:1, v/v) with Hex-NH_2 as the initiator, Trp-NCA as the monomer, and AcOH/DMAP as the catalyst. $[M]_0$ = 0.2 M, $[DMAP]_0/[I]_0$ = 1, $[M]_0/[AcOH]_0$ = 1. The monomers conversions were > 95% for all polymerizations as determined by FTIR. [b]Polymerization time reaching 95% monomer conversion. [c]Determined by GPC. d*n*/d*c* = 0.125.

Table S7. Characterization of resulting PLW from the polymerization of Trp-NCA in the presence of AcOH/DMAP at various monomer conversions.[a]

Entry	t (min)	$M_{n,\,GPC}$ (kDa)[b]	$Đ$ [b]
1	30	4.1	1.13
2	60	6.5	1.11
3	90	8.1	1.10
4	180	9.9	1.08

[a]All polymerizations were conducted at room temperature in DCM/DMF cosolvents (1:1, v/v) with Hex-NH_2 as the initiator, Trp-NCA as the monomer, and AcOH/DMAP as the catalyst. $[M]_0/[I]_0$ = 50, $[M]_0$ = 0.2 M, $[DMAP]_0/[I]_0$= 1, $[M]_0/[AcOH]_0$ = 1. [b]Determined by GPC; dn/dc = 0.125.

Table S8. Polymerization of Trp-NCA initiated by different amines in the presence of DMAP or AcOH/DMAP.[a]

Entry	Initiator	Additive	$M_{n,}$[b] $_{GPC}$ (kDa)[b]	$Đ$[b]
1	Pr-NH_2	DMAP	25.2	1.27
2[c]	Pr-NH_2	AcOH/DMAP	13.3	1.16
3	Bn-NH_2	DMAP	26.2	1.16
4[c]	Bn-NH_2	AcOH/DMAP	12.5	1.18

[a]All polymerizations were conducted at room temperature in DCM/DMF cosolvents with Trp-NCA as the monomer. $[M]_0/[I]_0$ = 50, $[M]_0$ = 0.2 M, $[DMAP]_0/[I]_0$= 1, $[M]_0/[AcOH]_0$ = 1. The theoretical MW was 9.4 kDa. The monomer conversion was > 95% for all polymerizations as determined by FTIR. [b]Determined by GPC; d*n*/d*c* = 0.125.

Table S9. Polymerization of Trp-NCA in the presence of DMAP/AcOH initiated by PEG_{2k}-NH_2.[a]

Entry	$[M]_0/[I]_0$	$M_{n,theo.}$ (kDa)	$M_{n,GPC}$ (kDa)[c]	$Đ$[c]
1	10	3.9	4.1	1.05
2	20	5.7	7.9	1.05
3	50	11.3	17.0	1.05
4	100	20.6	31.8	1.05

[a]All polymerizations were conducted at room temperature in DCM/DMF cosolvents (1:1, v/v) with PEG_{2k}-NH_2 as the initiator, Trp-NCA as the monomer, and AcOH/DMAP as the catalyst. $[M]_0$ = 0.2 M, $[DMAP]_0/[I]_0$= 1, $[M]_0/[AcOH]_0$ = 1. The monomer conversion was > 95% for all polymerizations as determined by FTIR. [b]Determined by GPC; dn/dc = 0.125.

Table S10. Synthesis of tryptophan-containing block copolypeptides in the presence of AcOH/DMAP.[a]

Entry	Copolypeptide	$M_{n,theo}$ (kDa)	$M_{n,GPC}$ (kDa)[b]	$Đ$[b]
1	E^{Bn}_{50}	11.1	10.0	1.13
2	E^{Bn}_{50}-*b*-W_{50}	20.3	23.3	1.05
3	E^{Bn}_{50}-*b*-W_{50}-*b*-E^{Bn}_{50}	29.7	30.3	1.05

[a]All polymerizations were conducted at room temperature in DCM/DMF cosolvents (1:1, v/v) with Hex-NH_2 as the initiator, Trp-NCA and BLG-NCA as the monomer, and AcOH/DMAP as the catalyst. $[M]_0$ = 0.2 M, $[DMAP]_0/[I]_0$= 1, $[M]_0/[AcOH]_0$ = 1. [b]Determined by GPC; d*n*/d*c* = 0.09-0.13.

Table S11. Synthesis of E^{tBu}-*co*-W copolypeptides in the presence of AcOH/DMAP.[a]

Entry	Sample	$M_{n,theo}$ (kDa)	$M_{n,GPC}$ (kDa)[b]	$Đ$[b]
1	E^{tBu}_{12}-*co*-W_{12}	4.6	5.9	1.05
2	E^{tBu}_{25}-*co*-W_{25}	9.4	11.3	1.05
3	E^{tBu}_{37}-*co*-W_{37}	13.8	16.7	1.05
4	E^{tBu}_{50}-*co*-W_{50}	18.7	20.5	1.05
5	E^{tBu}_{75}-*co*-W_{75}	27.9	30.0	1.07
6	E^{tBu}_{100}-*co*-W_{100}	37.2	36.0	1.08

[a]All polymerizations were conducted at room temperature in DCM/DMF cosolvents (1:1, v/v) with Hex-NH_2 as the initiator, Trp-NCA and tBuLG-NCA as the monomer, and AcOH/DMAP as the catalyst. $[M]_0/[I]_0$= 100, $[M]_0$ = 0.2 M, $[DMAP]_0/[I]_0$= 1, $[M]_0/[AcOH]_0$ = 1. [b]Determined by GPC; d*n*/dc = 0.09-0.13.

Table S12. Synthesis of K^{Boc}-*co*-W random copolypeptides using different NCA monomers in the presence of AcOH/DMAP.[a]

Entry	Sample	$M_{n,theo}$ (kDa)	$M_{n,GPC}$ (kDa)[b]	$Đ$[b]
1	K^{Boc}_{90}-*co*-W_{10}	22.5	21.0	1.06
2	K^{Boc}_{85}-*co*-W_{15}	22.3	23.2	1.05
3	K^{Boc}_{80}-*co*-W_{20}	22.1	23.0	1.06
4	K^{Boc}_{70}-*co*-W_{30}	21.6	23.7	1.07
5	K^{Boc}_{60}-*co*-W_{40}	21.2	21.8	1.08
6	K^{Boc}_{50}-*co*-W_{50}	20.8	20.7	1.09

[a]All polymerizations were conducted at room temperature in DCM/DMF cosolvents (1:1, v/v) with Hex-NH_2 as the initiator, Trp-NCA and BLL-NCA as the monomer, and AcOH/DMAP as the catalyst. $[M]_0/[I]_0 = 100$, $[M]_0 = 0.2$ M, $[M]_0/[AcOH]_0 = 1$, $[I]_0/[DMAP]_0 = 1$. [b]Determined by GPC; d*n*/dc = 0.070-0.098.

Table S13. Polymerization of Trp-NCA in the presence of AcOH/DMAP with monomers of different chiralities.[a]

Entry	$[M]_0/[I]_0$	t (h)[b]	$M_{n,theo.}$ (kDa)	$M_{n,GPC}$ (kDa)[c]	$Đ$[c]
1	50	3	9.4	9.6	1.1
2	75	3	14.1	15.6	1.07
3	100	4	18.7	19.1	1.07
4	150	6	28.0	29.5	1.05
5	200	8	37.3	38.0	1.05
6[d]	50	7	9.4	11.8	1.09

[a]All polymerizations were conducted at room temperature in DCM/DMF cosolvents (1:1, v/v) with Hex-NH_2 as the initiator, $_D$-Trp NCA as the monomer, and DMAP as the catalyst. $[M]_0$ = 0.2 M, $[DMAP]_0/[I]_0$ = 1. The monomers conversions were > 95% for all polymerizations as determined by FTIR. [b]Polymerization time reaching 95% monomer conversion. [c]Determined by GPC. dn/dc = 0.125. [d]$_{DL}$-Trp NCA was used as monomer.

Cartesian Coordinates of the optimized geometries

Int1

C	-2.49621500	-0.05955600	-0.39254600
C	-3.23471100	1.07543500	0.06234900
C	-4.58377500	0.98487000	0.43185500
C	-5.19539500	-0.26420100	0.34459800
C	-4.48357000	-1.39969600	-0.10359000
C	-3.14389000	-1.30793800	-0.47262100
C	-1.15843600	0.39719900	-0.68595900
C	-1.13985200	1.74689400	-0.40466400
H	-5.13504200	1.86259200	0.77635300
H	-6.24586600	-0.36707900	0.62728900
H	-4.99614000	-2.36297200	-0.16132300
H	-2.60568200	-2.19252700	-0.82298500
H	-0.31715800	2.45465700	-0.48404200
C	-0.00908600	-0.43692800	-1.15066300
H	-0.31523500	-1.06928600	-2.00144900
H	0.83205200	0.18934300	-1.47725900
C	0.53522500	-1.39775600	-0.06771400
C	1.20828800	-0.68586600	1.09720800
H	-0.29216000	-2.00466200	0.33863900
C	2.78556400	-1.99786500	0.12027300
O	0.75634800	0.11369700	1.86224400
O	2.50467000	-1.12425100	1.17537000
O	3.89424800	-2.42041400	-0.07422100
N	1.62689000	-2.22801000	-0.53277900
H	1.60717400	-2.76605500	-1.39143000
N	-2.37871200	2.15382100	0.04055100

H	-2.62150700	3.10152200	0.30023600
N	3.10960700	0.91914200	-0.93712500
H	3.13029700	1.30857500	-1.88140500
C	3.16737200	1.99827500	0.04901000
H	2.24085700	2.59152400	-0.04075800
H	3.13528500	1.54107600	1.05122400
C	4.38146900	2.92004200	-0.06082400
H	4.35891100	3.70712200	0.71111100
H	5.31878900	2.35187500	0.06297600
H	4.41529100	3.41402000	-1.04657100
H	3.94558100	0.33590000	-0.86256600

Int2

C	-2.19560300	-0.31535700	-0.35388000
C	-3.20826900	0.64426600	-0.04647300
C	-4.42801000	0.27992600	0.54085100
C	-4.63580300	-1.06993100	0.81502400
C	-3.65387800	-2.03845800	0.50789100
C	-2.44162600	-1.67434200	-0.07226300
C	-1.09085600	0.40802700	-0.94436000
C	-1.47563200	1.73182700	-0.97920100
H	-5.18903400	1.02891400	0.77085200
H	-5.57660900	-1.38571100	1.27233900
H	-3.85239800	-3.08977600	0.72975600
H	-1.69593000	-2.43691200	-0.30902400
H	-0.93961900	2.59796400	-1.35947200
C	0.19110200	-0.18974500	-1.44543900
H	-0.04575800	-0.94860400	-2.21233800

H	0.81499900	0.56379300	-1.94666000
C	1.01230000	-0.90789200	-0.37103900
C	1.89296800	-0.03968000	0.58472100
H	0.33072600	-1.47891800	0.28138900
C	3.09182300	-1.91626200	-0.09160800
O	1.17363800	0.17969600	1.73601100
O	3.01983100	-0.93525300	0.84793100
O	3.98839300	-2.72675800	-0.13007700
N	2.02712700	-1.78259700	-0.93283900
H	1.79401700	-2.54641900	-1.55759200
N	-2.73703400	1.87501500	-0.44138400
H	-3.23554600	2.75133700	-0.35316700
N	2.49924300	1.16536100	0.12027700
H	3.17956800	0.99890500	-0.61549700
C	1.74423500	2.40383800	-0.03659700
H	1.41165600	2.55318200	-1.08014700
H	0.83219700	2.32167300	0.56961700
C	2.56080800	3.61312900	0.40876100
H	1.98588300	4.54353700	0.27521300
H	2.84308400	3.52275800	1.46943100
H	3.48800000	3.70146700	-0.18077700
H	1.69316200	0.78077900	2.29444600

Int3

C	1.46817500	-0.80942900	-0.93639600
H	1.33720200	-1.13149600	-1.98198200
H	1.84563900	0.21887500	-0.94264900
C	2.54698800	-1.69611900	-0.30609400

C	2.98540000	-1.26692600	1.09122800
H	2.17890900	-2.73589400	-0.22524200
C	4.84493500	-1.26122800	-0.21352900
O	2.32441300	-1.12598700	2.07995500
O	4.34149100	-1.10518000	1.08518900
O	6.00359500	-1.07468600	-0.46879500
N	3.81675800	-1.64198400	-0.99988100
H	3.93641700	-1.79288500	-1.99471000
C	0.13190600	-0.87509600	-0.20485300
H	0.27769300	-0.69602200	0.87365400
H	-0.34210100	-1.86494600	-0.28619700
C	-0.84100300	0.17560600	-0.68618700
C	-3.12587500	0.81214900	-0.72852300
H	-3.13235100	0.95195600	-1.81937900
H	-2.86185800	1.77422600	-0.26508800
C	-4.44225600	0.29331000	-0.22635900
C	-4.79473900	0.44979700	1.12274000
C	-5.31964700	-0.38232600	-1.08556800
C	-6.00234100	-0.06023200	1.60413600
H	-4.11610900	0.97688700	1.79861800
C	-6.53079400	-0.89111300	-0.60738900
H	-5.05197200	-0.50817000	-2.13798100
C	-6.87320500	-0.73184300	0.73873800
H	-6.26777000	0.06930700	2.65604500
H	-7.20859400	-1.41255800	-1.28736200
H	-7.81998800	-1.12788900	1.11371400
O	-2.10458500	-0.15542400	-0.38994400
O	-0.53951300	1.20971000	-1.24202700

N	3.21167600	1.60990500	0.48637700
H	4.19401400	1.74826400	0.73023200
C	2.72227200	2.73435700	-0.31244200
H	3.29481500	2.75232800	-1.25595800
H	1.67784900	2.51989700	-0.59524200
C	2.80643300	4.10192300	0.36549500
H	2.42406400	4.90022000	-0.29216800
H	2.21235400	4.11694900	1.29493900
H	3.84854000	4.35006200	0.62858400
H	2.71350900	1.57100900	1.37769400

Int4

C	1.44777400	-0.99255800	-0.71487400
H	1.28098300	-1.94145800	-1.24947000
H	1.69028000	-0.24570200	-1.48310400
C	2.63408900	-1.17115000	0.22023000
C	3.29975600	0.14171200	0.75911300
H	2.32161000	-1.75128200	1.10730500
C	4.95400800	-1.35675400	0.09843200
O	2.79940700	0.37943700	2.01962200
O	4.70664200	-0.23685600	0.83172200
O	6.06249500	-1.81710300	-0.04489800
N	3.77406700	-1.79805700	-0.42182400
H	3.72589200	-2.72780100	-0.82333000
C	0.17016700	-0.60877400	0.02908300
H	0.37157600	0.17185700	0.78157500
H	-0.24159800	-1.45881400	0.59217700
C	-0.90130100	-0.05378800	-0.87997700

C	-3.22875900	0.34773500	-1.10310100
H	-3.23895600	-0.10518600	-2.10516300
H	-3.06077700	1.42833200	-1.22059100
C	-4.49246800	0.05773800	-0.34654100
C	-4.97153400	0.96258200	0.61168400
C	-5.18856900	-1.14089800	-0.56029700
C	-6.12731900	0.67621700	1.34289900
H	-4.43460000	1.89930600	0.78319300
C	-6.34416200	-1.43032500	0.16960500
H	-4.82150000	-1.85072600	-1.30635800
C	-6.81514900	-0.52166200	1.12317100
H	-6.49352900	1.39008300	2.08449700
H	-6.88030400	-2.36569100	-0.00742500
H	-7.72039500	-0.74561200	1.69257200
O	-2.12252700	-0.21260100	-0.35582700
O	-0.69855900	0.50371900	-1.93726800
N	3.28432200	1.33097500	-0.03241400
H	3.76141200	1.20085700	-0.92104700
C	2.10638900	2.19066000	-0.13384000
H	1.36374000	1.82299800	-0.86494400
H	1.60762500	2.19587700	0.84590800
C	2.51553700	3.61137500	-0.50617300
H	1.63118800	4.26388000	-0.57602200
H	3.20601400	4.02892400	0.24283500
H	3.02364100	3.63113200	-1.48447300
H	3.16854900	1.22316600	2.32823500

TS1

C	-2.17691800	-0.26030700	-0.40585600
C	-3.18721500	0.67754600	-0.03063600
C	-4.39730100	0.27902800	0.55461900
C	-4.59873700	-1.08374800	0.75837800
C	-3.61988100	-2.03126000	0.38340200
C	-2.41769500	-1.63294100	-0.19438200
C	-1.08433600	0.49977400	-0.97170300
C	-1.47544700	1.82240000	-0.92950400
H	-5.15503200	1.01334800	0.83669700
H	-5.53160200	-1.42640500	1.21257400
H	-3.81262000	-3.09368400	0.55042400
H	-1.67662000	-2.38116700	-0.48412800
H	-0.95482600	2.71032700	-1.28261100
C	0.20008300	-0.03798900	-1.53109600
H	-0.03024400	-0.72043800	-2.36938700
H	0.80385700	0.76850100	-1.96427800
C	1.02908900	-0.87073100	-0.54820600
C	1.58943000	-0.27765600	0.75971900
H	0.38011300	-1.68287600	-0.17329900
C	3.12380900	-1.78215700	-0.15693300
O	0.77446700	-0.13272100	1.78626800
O	2.72985700	-1.20736600	1.00915800
O	4.10887800	-2.47702300	-0.25641900
N	2.23787800	-1.42422500	-1.13732300
H	2.21548100	-1.97151800	-1.99138100
N	-2.72778700	1.93046000	-0.36408800
H	-3.23058200	2.79756400	-0.22430900
N	2.26555700	1.10130900	0.82960000

H	3.25603100	0.97410500	1.05577100
C	2.08559000	2.18248300	-0.15228300
H	2.52787900	1.88824000	-1.11653800
H	1.00800900	2.32184900	-0.29403900
C	2.72065300	3.46711200	0.35926400
H	2.56889300	4.27654300	-0.36994600
H	2.27141800	3.77363200	1.31636300
H	3.80543600	3.34527900	0.50909200
H	1.47252000	0.98143400	1.81093100

TS2

C	1.36155700	-0.86582000	-0.89228600
H	1.15588900	-1.71050900	-1.56960300
H	1.56275700	-0.00364800	-1.53650700
C	2.58484000	-1.22699800	-0.06222400
C	3.15453900	-0.21361900	0.95175700
H	2.31525500	-2.08903400	0.57909600
C	4.89638600	-1.37096600	-0.06868200
O	2.53415500	-0.07805500	2.11564900
O	4.55413900	-0.67930700	1.05431700
O	6.02144500	-1.74909600	-0.29526300
N	3.77574600	-1.52512300	-0.83928300
H	3.78110400	-2.23322600	-1.56600800
C	0.12999700	-0.60584300	-0.01929100
H	0.42250700	-0.05435600	0.89118900
H	-0.32624000	-1.54084000	0.33420300
C	-0.91503200	0.23535500	-0.71139700
C	-3.23153500	0.72797800	-0.84679800

H	-3.21611600	0.64498400	-1.94320900
H	-3.05042500	1.78016800	-0.58269200
C	-4.51918000	0.21957700	-0.26649000
C	-5.00430900	0.73271100	0.94517000
C	-5.23306300	-0.80259600	-0.90846900
C	-6.18337200	0.23450800	1.50531100
H	-4.45355600	1.53013400	1.45106800
C	-6.41247000	-1.30285700	-0.35083200
H	-4.86116400	-1.20698300	-1.85361900
C	-6.88919900	-0.78490500	0.85786500
H	-6.55394400	0.64392100	2.44804000
H	-6.96229900	-2.09707000	-0.86132100
H	-7.81275800	-1.17346300	1.29364900
O	-2.15204300	-0.07396600	-0.30899500
O	-0.67543400	1.12067800	-1.50593600
N	3.30681400	1.28488800	0.62955400
H	4.30450100	1.51468000	0.65266000
C	2.63877800	2.01832800	-0.46143100
H	3.01180900	1.65776100	-1.43271300
H	1.56177900	1.81568800	-0.41888200
C	2.89441200	3.51118900	-0.31205300
H	2.38484500	4.05946500	-1.11799000
H	2.51391900	3.88038900	0.65275800
H	3.97013800	3.74255300	-0.37180800
H	2.78188400	1.16273400	1.78070800

Reference

[1] Tian, Z. Y.; Zhang, Z.; Wang, S.; Lu, H. A moisture-tolerant route to unprotected *α*/*β*-amino acid *N*-carboxyanhydrides and facile synthesis of hyperbranched polypeptides. *Nat. Commun*. **2021,** *12*, 5810.

[2] Sun, X.; Li, A.; Li, N.; Ji, G.; Song, Z. Facile preparation of heteropolypeptides from crude mixtures of *α*-amino acid *N*-carboxyanhydrides. *Biomacromolecules*. **2024,** *25*, 6093-6102.

[3] Denisov, M.; Gorbunov, A.; Dmitriev, M. V.; Slepukhin, P.; Glushkov, V. Synthesis and Structure of Ferrocenol Esters. *Int. J. Org. Chem.* **2016,** *06*, 107-116.

[4] Sheldrick, G. M. Crystal structure refinement with SHELXL. *Acta Crystallogr C Struct Chem*. **2015,** *71*, 3-8.

[5] Sheldrick, G. M. A short history of SHELX. *Acta Crystallogr A*. **2008,** *64*, 112-122.

[6] Guo, C.; Li, C.; Vu, H. V.; Hanna, P.; Lechtig, A.; Qiu, Y.; Mu, X.; Ling, S.; Nazarian, A.; Lin, S. J.; Kaplan, D. L. Thermoplastic moulding of regenerated silk. *Nat. Mater*. **2020,** *19*, 102-108.

[7] Kamada, A.; Rodriguez-Garcia, M.; Ruggeri, F. S.; Shen, Y.; Levin, A.; Knowles, T. P. J. Controlled self-assembly of plant proteins into high-performance multifunctional nanostructured films. *Nat. Commun*. **2021,** *12*, 3529.

[8] Koch, S. A.; Doyle, T. D. Direct determination of amine salt-base ratios by nuclear magnetic resonance spectrometry: correlation of acid strengths in chloroform by nuclear magnetic resonance and infrared spectrometry. *Anal. Chem*. **1967,** *39*, 1273-1276.

[9] Frisch, M. J.; Trucks, G. W.; Schlegel, H. B.; Scuseria, G. E.; Robb, M. A.; Cheeseman, J. R. et al. Gaussian 16, Revision C.01, Gaussian, Inc., Wallingford CT, **2016**.

[10] Becke, A. D. Density-functional exchange-energy approximation with correct asymptotic behavior. *Phys. Rev. A* **1988**, 38, 3098–3100.

[11] Lee, C.; Yang, W.; Parr, R. G. Development of the Colle-Salvetti correlation-energy formula into a functional of the electron density. *Phys. Rev. B* **1988**, 37, 785–789.

[12] Becke, A. D. Density-functional thermochemistry. III. The role of exact exchange. *J. Chem. Phys.* **1993**, 98, 5648–5652.

[13] Grimme, S.; Antony, J.; Ehrlich, S.; Krieg, H. A consistent and accurate *ab initio* parametrization of density functional dispersion correction (DFT-D) for the 94 elements H–Pu. *J. Chem. Phys.*, **2010**, 132, 154104.

[14] Grimme, S.; Ehrlich, S.; Goerigk, L. Effect of the damping function in dispersion corrected density functional theory. *J. Comput. Chem.*, **2011**, 32, 1456–1465.

[15] Weigend, F.; Ahlrichs, R. Balanced basis sets of split valence, triple zeta valence and quadruple zeta valence quality for H to Rn: Design and assessment of accuracy. *Phys. Chem. Chem. Phys.*, **2005,** 7, 3297–3305.

[16] Miertuš, S.; Tomasi, J. Electrostatic interaction of a solute with a continuum. A direct utilization of ab initio molecular potentials for the prevision of solvent effects. *Chem. Phys. Lett.* **1982**, 93, 229–234.

[17] Legault, C. Y. CYLview, 1.0b. Université De Sherbrooke, 2009, http://www.cylview.org.